A Topology Optimized Model based on the Level-Set Method for Porous Bone Scaffolds

Bahar Imanlou

Submitted to the Graduate School of Engineering and Natural Sciences

in partial fulfillment of the requirements for the degree of

Master of Science

Sabanci University

August, 2016

TITLE OF THE THESIS/DISSERTATION

APPROVED BY:

Assoc. Prof. Dr. Güllü Kızıltaş Şendur.....
(Thesis Supervisor)

Prof. Dr. Bülent Çatay.....

Assoc. Prof. Dr. Çetin Yılmaz.....

DATE OF APPROVAL:..07.09.2016...

A Topology Optimized Model based on the Level-Set Method for Porous Bone Scaffolds

Bahar Imanlou

Industrial Engineering, Master's Thesis, 2016

Thesis Supervisor: Güllü Kızıltaş Şendur

Abstract

In a well-designed porous scaffold, there is a need for a convenient balance between biological compatibility and mechanical functionality such that the porosity permits tissue regeneration and solid structure carries the load in the best possible way. In this thesis, a design framework that allows for the optimal design and analysis of a bone scaffold which undergoes tissue regeneration according to a self healing model is proposed. Computational models are implemented using COMSOL Multiphysics which provides the opportunity to build an FEA (Finite Element Analysis) model where boundary value problems from different disciplines and mathematical equations are coupled and studied at the same time to reach an optimally performing tissue. To simulate the self healing process a mechano-regulatory model is developed mimicking tissue regeneration. As the topology optimization design method, level-set method is employed, where the design process starts with an initial geometry, that satisfies physical constraints. At each time step, this geometry is improved based on sensitivity analysis results until convergence is reached. Results of both the mechano-regulatory and the topology optimization methods validate well-known benchmark design problems in literature. Finite element method integrated to the level-set based topology optimization is proven to be among the most computationally efficient and generic design tool for solving non-intuitive tissue engineering problems. Hence, the proposed design framework, when implemented with corresponding physical models, is equally applicable to other hard and soft tissue designs.

Gözenekli Kemik Doku İskelesi için Level Set Yöntemine dayalı Topoloji Optimizasyonu

Bahar Imanlou

Endüstri Mühendisliği, Yükseklisans Tezi, 2016

Tez Danışmanı: Güllü Kızıltaş Şendur

Özet

İyi tasarlanmış gözenekli bir kemik doku iskelesinde, biyolojik uyum ve mekanik fonksiyonellik arasındaki dengeyi sağlayacak bir yapıya ihtiyaç duyulmaktadır. Bu duruma, hem gözenekli yapının yeniden doku oluşturması hem de yükün sağlam yapı tarafından olası en iyi şekilde taşınmasını sağlayan dengeli tasarımdaki ödünleşim örnek olarak verilebilir. Bu tezde, kendi kendini iyileştirme modeline göre doku yenilenmesine uğramış kemik iskelesinin optimal tasarımına ve analizine olanak sağlayan bir çalışma sunulmuştur. Hesaplamalı modeller, sonlu elemanlar analiz modeli (FEA) oluşumuna olanak sağlayan COMSOL Multiphysics kullanılarak kurulmuştur. Geliştirilen FEA modeli, dokunun optimal yapıya ulaşmasını amaçlarken, farklı disiplinlere ait sınır değer problemlerinin ve matematiksel denklemlerin birleştirildiği ve aynı anda çalışılmasına dayanır. Kendi kendine iyileştirme modellerini simüle edebilmek için, doku yenilenmesini taklit eden 'mechano-regulatory' modeli geliştirilmiştir. Topoloji optimizasyon modelinde tasarım süreci, fiziksel kısıtları sağlayan rastgele bir başlangıç geometrisi ile başlar ve 'level-set' metodunu kullanır. Bu geometri yakınsama sağlanana kadar, her zaman diliminde duyarlılık analizine göre güncellenerek iyileştirilir. Topoloji optimizasyonu ve 'mechano-regulatory' yöntemlerinin sonuçları, literatürde bilinen problemlerin sonuçları ile doğrulanmıştır. 'Level-set' bazlı topoloji optimizasyonu ile birleştirilmiş olan sonlu elemanlar yönteminin, sezgisel olmayan doku mühendisliği problemlerinin çözümünde en verimli ve kapsamlı tasarım aracı olduğu kanıtlanmıştır. Bu nedenle, önerilen tasarım çerçevesi, fiziksel modeller uygun olduğunda, diğer sert ve yumuşak doku tasarımlarında da eşit derecede uygulanabilecek özelliktedir.

to my beloved family

Acknowledgements

I would like to express my gratitude to my advisor, Prof. Güllü Kızıltaş Şendur, for her endless patience and immense knowledge. I would also like to appreciate the rest of my thesis jury members: Prof. Bülent Çatay and Prof. Çetin Yılmaz, for their insightful comments and advices. I would like to thank my wonderful friends: Sahar, Raha, Maboo, Bahar, Mahsa, Reihoon, Moreno, Carlos, Joe, Oreo, Deniz, Ali, Szilvi, Gizem, Ece, Murat, Özgün, Osman, Omid, Sonia, Faran, Yağmur, Sinem, Zeynep and Yelda. Thank you for making time for me and accepting me at my best and my worst. You are the most precious gifts that I ever received and I am forever grateful. Finally, I would like to thank my family for their endless support and love. Dear Mom, everything I have done is nothing compared to what you did and sacrificed for me. I love you.

Contents

List of Figures

List of Tables

1 Introduction

1.1 Motivation and Objective

The skeletal system is an important part of the body especially when biomechanism and metabolism are considered. Within the skeletal system, bone has a complicated structure along with high rigidity and hardness that makes it very different from other tissues. After fracture, bone shows an amazing ability to heal itself but in many cases if self curing is not possible, a scaffold is used to fill the gap. No self-healing situation might result from diseases and injuries or could be congenital. A common approach to bone replacement problems, consists of these steps:

1. Imaging defect using CT or MRI
2. Designing a proper replacement
3. Fabrication of the model using additive manufacturing techniques

This thesis focuses on the second step of designing a bone scaffold and its self-healing process. A very crucial task in designing the scaffold is the interior porous part which is required to be as similar as possible to the original intricate structure of bone. Most of the design studies in literature proposed for bone scaffold designs rely mainly on experimental techniques or trial and error based efforts. However to satisfy the stringent multifunctionalities of a bone scaffold, this complicated structural search needs to rely on formal and robust design methodologies such as topology optimization. Topology optimization based design results were presented mainly by Hollister (2005) and his research group incorporating various behaviors of

the bone scaffold such as strength, elasticity, diffusion, permeability, angiogenesis and manufacturability. More specifically, they have used Finite Element Analysis (FEA) based Solid Isotropic Material with Penalization (SIMP) and homogenization based topology optimization approaches to come up with novel scaffold designs. These designs were also fabricated by the same group using advanced 3D fabrication methods such as Indirect Solid Freeform Fabrication or 3D Inkjet printing. To overcome well known problems of standard topology optimization approaches such as gray scale issues and checkerboard problems, more recently, alternative topology optimization based on the level-set method was proposed by Osher and Sethian (1988) and applied applied to mechanical (Allaire et al. (2005)), fluid-flow and electromagnetic applications. Here, in this thesis a level-set based topology optimization will be applied for the first time to bone scaffold design problems. As stated earlier besides mechanical strength, biological functionality needs to be considered in designing a fully functional bone. In literature, the biological functionality of the bone has been simulated via different computational models. Among them, very similar to topology optimization, mechanoregulation as proposed by Prendergast et al. (1997) relies on FEA models. Therefore it is chosen to be applied in this thesis to mimick the biological response of the bone scaffold. In short, as a starting pont, the mechano-regulatory model relying on stimuli driven by mechanical strain and fluid velocity will be implemented in its simple form as proposed by Prendergast et al. (1997). At the end, the two models, namely mechano-regulatory model and the level set based topology optimization design approach will be integrated.

Hence, the objective of this thesis is to develop a versatile and modular design framework that is capable of mimicking both biological functionality -via the mechano-regulatory model-and optimal mechanical response of a bone scaffold via the level set based topology optimization model.

1.2 Contributions

Most of the bone scaffold design problems in literature as summarized in Section 1.1 and will be presented in more detail in Chapter 2 are either experimentally driven or rely on trial and error studies. Very few studies are based on formal optimization studies. Most notable studies are done by Hollister et al. (2002) and Hollister (2005) where a 3D structure with

cylindrical pores was optimized in terms of porosity and material through an image-based homogenization optimization approach. In this thesis, in order to arrive at a non-intuitive multi-functional bone scaffold that delivers among other mechanical strength and biological self-healing requirements, a mechanical topology optimization design framework based on the level set method is developed. More specifically, first, a structure based on a model simulating the natural self-healing process of a bone undergone fracture is simulated. Then, a compliance minimization technique to achieve an optimized scaffold instead of self-healing model is studied. The contribution of this thesis are as follows:

- the implementation of a mechano-regulatory model based on Prendergast et al. (1997) in a COMSOL Multi-physics environment
- the development of a topology optimization design framework based on the level set method for compliance minimization of bone scaffolds

2 Preliminaries and Background

2.1 Structure and Properties of Bone

The complexity of bone's properties arises from the complexity in its structure. Bone is an anisotropic, heterogeneous, inhomogeneous, nonlinear, thermorheologically complex viscoelastic material. At the microstructural level, fibers of 3 to 5 μm thick are either randomly arranged and form *woven bone* or organized into concentric lamellar groups and make *osteons* or linear layered groups as *plexiform bone*. Combinations of these tissues make two different types of bones in terms of architectural structure, a strong, stiff and dense type called *cortical bone* found in shaft of long bones and a spongy called *trabecular bone* found in the end of long bones, ribs and skull(Figure 1). At the macrostructural level we have the whole bone and the properties is a result of properties of smaller parts.

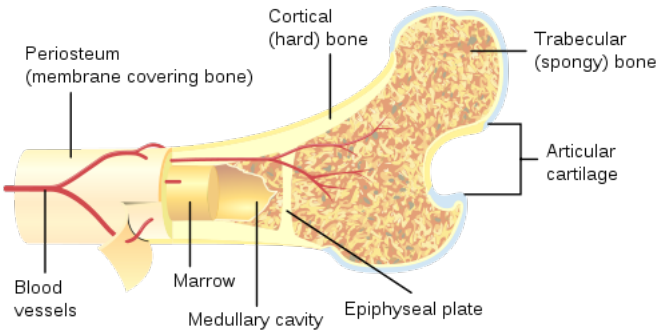

Figure 1: Cross-section of a bone showing cortical and trabecular tissues

In this thesis, we are studying a fracture in middle part of tibia, where there exist only cortical bone. In addition to that, the porous structure is filled with interstitial fluid which is a combination of many different materials, mainly consisting of plasma and blood.

2.2 Mechano-regulatory Model

Mechanical loading has a great influence on the process of bone healing. Many biomechanical fracture healing studies bith experimental Aro and Chao (1993) Claes et al. (1998) and clinical Goodship and Kenwright (1985) Goodship et al. (1998) Kenwright and Gardner (1998) show that inadequate mechanical stimulation slows down the initial stage of healing while excessive amount of it prevents ossification and causes instability. Mechano-regulatory Model introduced by Huiskes et al. (1997) Prendergast et al. (1997) is an iterative algorithm modeling the process of fracture healing in bones considering it a solid linear elastic material. The model has successfully simulated tissue differentiation during fracture healing for various clinical cases. The stability of the algorithm and the use of fixed input parameters throughout the study, indicate that this concept may be applied to other problems in mechanobiology Huiskes et al. (1997). In Prendergast's model distortional strain γ and fluid velocity u are the main biophysical stimuli for stem cell differentiation and these are used to calculate stimulus S which defines the new cell type.

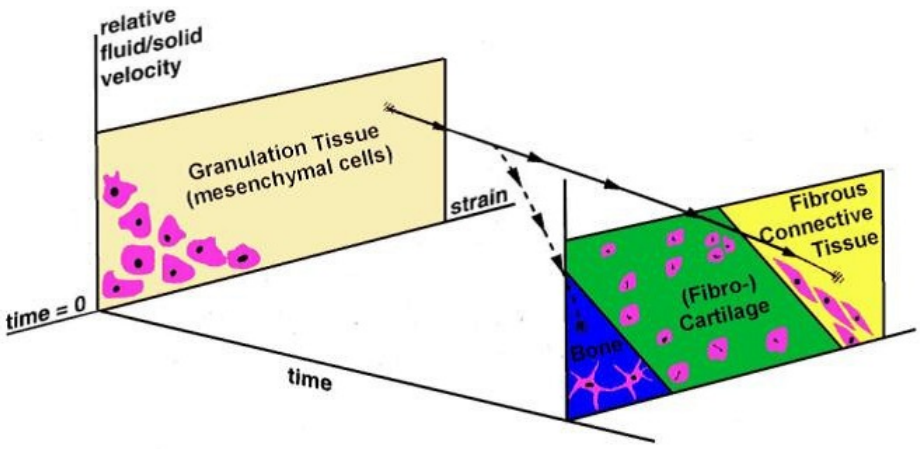

Figure 2: Schematic of the mechano-regulation model proposed by Prendergast et al. (1997)

As shown in Figure 2 , stem cells would emerge to either bone(blue), cartilage(green) or fibrous connective tissue(yellow) based on the calculated value of S. If, as a result of high shear strain and fluid flow, a high stimuli is maintained(full line), stem cells will differentiate into fibrous connective tissues. On the other hand, if the stimuli is decreased(dashed line)

bone starts to form.

2.3 Topology Optimization

Topology optimization is a relatively new but rapidly growing field, which has theoretical foundations and applications in mechanics, mathematics, computer science and manufacturing fields such as car and aerospace industries. The basic idea behind topology optimization in a mechanical structure is to minimize(or maximize) one or several features of that structure while satisfying boundary conditions. For example, a compliance minimization problem (stiffest structure) for a linear elastic system with given fixed supports and a prescribed external loading f can be written as:

$$\begin{aligned} min: \quad & C = f_p^T u_p \\ s.t. \quad & K(\rho)u = f && \text{(1a)} \\ & \sum_{e=1}^{N} \rho_e v_e \leq V^* && \text{(1b)} \end{aligned}$$

In the first paper on topology optimization, Michell (1904) derived optimality criteria for minimum weight layout of trusses. Later, his work was extended to other problems such as grillages,Rozvany (1972a), flexuresRozvany (1972b) and some some popular benchmark problems Rozvany (1998). Starting in late 80's, after Bendsøe (1989) redefined the problem as a material distribution one, many researchers have been studying numerical methods for topology optimization problemsRozvany (2001). There are different methods of approaching topology optimization problems. One of the first commonly used solvers, called *homogenization*, is based on a large number of predefined microstructures Bendsøe and Kikuchi (1988). Another popular approach is *solid isotropic microstructures with penalization* ($SIMP$) Bendsøe and Sigmund (1999) also know as *material interpolation*, *powerlaw* or *density* method. Other approaches such as the on-off approach solved via *integerprogramming* or *geneticalgorithms*, are also discussed in many papers. Each of these methods have their advantages and limitations. GA and discrete methods via the on-off ap-

proach is by definition an ill-posed problem. In other words the optimum topology changes when the discretization of the structure changes. SIMP and other continuous design models overcome this problem by introducing a grey scale material choice instead of the black/white or on/off and mapping it to a simple and effective continuous variable called the density. However these type of methods are known to suffer from checkerboard and grey scale problems in the final design. Level set method was introduced to overcome some of these problems and is discussed next.

2.4 Level set Method

Level set method was first introduced in 1988 by Osher and Sethian (1988) for capturing moving fronts. As shown in Figure 3, in this method, a surface is used to represent a flat shape. The surface is called level set function and its zero level set (black curve) shows the original shape. Imagine we have two different phases of materials shown with dark and light gray and we are interested in moving boundary between them. Since separation and merging could happen within either of these phases, we will have a topological change that is quite hard to parameterize whereas it's easy to represent it with the level set function. That is why this method is known to be a very strong technique to track the motion of an interface.

Since its introduction, level set method has been investigated in several papers as how to couple the finite difference method (FDM) and finite element method (FEM) to solves physical problems and the level set function Sethian and Wiegmann (2000)Osher and Santosa (2001)Allaire et al. (2005). In most cases, the optimization procedure is implemented by iterations of consecutively coupled solvers for the physical problems and the level set function.

2.5 Finite Element Method

In this section the FEM which is the backbone of the analysis tool used in this thesis is introduced shortly. The finite element method (FEM) or finite element analysis (FEA) is a numerical technique for obtaining approximate solutions for partial differential equations(PDEs). FEM splits a large and continuous problem into discrete parts (finite elements) with sim-

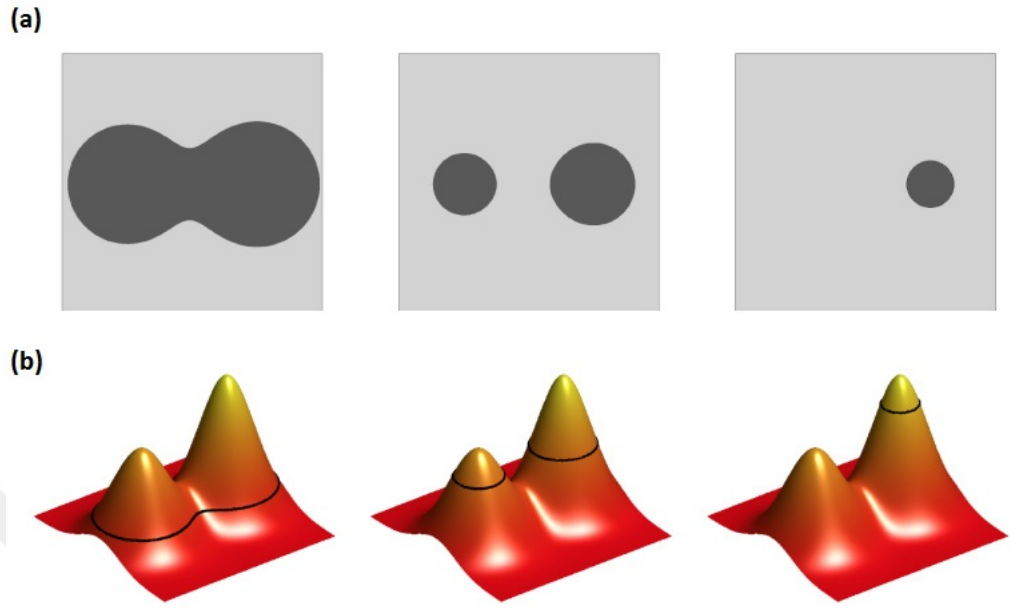

Figure 3: Three sets of 2D shapes(a) and their representing level set functions(b)

pler equations. These simple equations are then assembled into a larger system of equations that governs the entire problem. Then, it approximates a solution using variational methods. More details on this very well known approximate solution technique can be found in literature Zienkiewicz et al. (1977) Bathe (2006) Hughes (2012). FEA has been chosen as the main platform of this study because we will be dealing with different PDEs. More specifically, the following modules were employed and solved via FEA: the ”Steady State Solid Mechanics” module designed for linear elastic model was used to solve the displacement response of 2D structures and the generalized PDE was used to solve the Hamilton Jacobi Equation of the level set formulation. FEM is implemented via the commercial software COMSOL which not only allows the analysis of boundary value problems from different domains such as fluid-flow, mechanics and electromagnetic, but also has an interface for MATLAB coding. The design framework developed in this thesis was therefore implemented in COMSOL Multiphysics integrated to MATLAB interface.

2.6 COMSOL Multiphysics and LiveLink

COMSOL Multiphysics is a comprehensive finite element analysis software providing many modules for various physics and engineering applications, especially coupled phenomena, or multiphysics. In addition to the built-in modules, COMSOL Multiphysics also provides a framework to define user written systems of partial differential equations. These partial differential equations can be registered directly or using the weak form. COMSOL LiveLink is a connection between COMSOL and MATLAB allowing the user to control the FEA accessing the process steps with MATLAB. The combination of COMSOL Multiphysics and LiveLink is a perfect tool to solve the problem defined by this thesis as it is possible to solve PDE's from different fields related to the scaffold structure response such as mechanical and fluid flow as well as bone rehealing and link these using the proposed algorithm in LiveLink interface.

3 Methodology and Simulation Setup

3.1 Mechano-regulatory Based Generated Model

In this chapter, based on Lacroix et al. (2002) a transverse fracture creating 10mm gap in shaft of human tibia will be studied. A simplified 2D axisymmetric representation(Figure 4) is showing the top half of fracture including the broken bone and inserted granulation cells. Whole domain is a porous structure filled with interstitial fluid. An axial ramped loading of 500kN/m is applied in cycles and results are being stored at the end of each iteration.

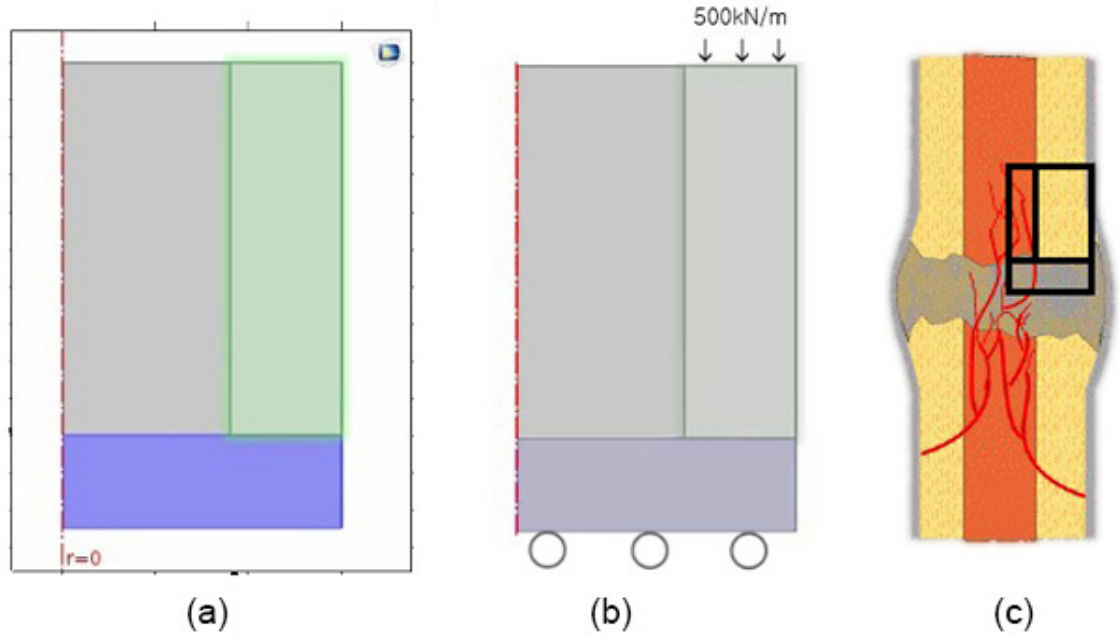

Figure 4: (a)Studied mechanoregulatory model consisting of fractured bone(green), granulation cells(blue) and marrow(grey) cells. (b)Boundary Conditions. (c)Attribution to real bone fracture.

This fracture and related cells were modeled as a poroelastic system in COMSOL Multiphysics with the following set of equations:

$$-\nabla.\sigma = F_v \tag{2}$$

$$\rho S \frac{\partial pf}{\partial t} + \nabla.(\rho u) = Q_m - \rho \alpha_B \frac{\partial e_{vol}}{\partial t} \tag{3}$$

$$u = -\frac{\kappa}{\mu} \nabla p_f \tag{4}$$

Where σ is the stress tensor, F_v is the body force, ρ is the density, S is the compliance, pf is the fluid pressure, t is time, u is the displacement, Q_m is the mass source, α_B is the Biot-Willis coefficient, e_{vol} is the porosity, κ is the permeability, μ is the dynamic viscosity. Implementation of these equations in COMSOL is achieved within the Time dependent Poroelastic module. Initially gap is filled with granulation tissuePrendergast et al. (1997) which, gradually differentiate to other types such as bone, cartilage or fibrous connective tissue, based on the following equations.

Octahedral shear strain is given by:

$$\gamma_{oct} = \frac{2}{3} \sqrt{(\varepsilon_1 - \varepsilon_2)^2 + (\varepsilon_1 - \varepsilon_3)^2 + (\varepsilon_3 - \varepsilon_2)^2} \tag{5}$$

where ε_1, ε_2 and ε_3 are the principal strain tensors and fluid velocity is:

$$u_f = \sqrt{u_r^2 + u_z^2} \tag{6}$$

where u_r and u_z are radial and axial components of Darcy's velocity field.

At the peak of each loading cycle(final time step), values of fluid velocity and strain in each node is stored and used to calculate mechanical stimuli in the corresponding point.

Stimulus S is calculated as:

$$S = \frac{\gamma_{oct}}{a} + \frac{u_f}{b} \tag{7}$$

where $a = 0.0375$ and $b = 3\mu m/s$ are empirical constantsPrendergast et al. (1997).

Using a MATLAB script written to control this model, first the poroelastic module is computed and values of stimuli in each node is stored to determine new tissues of that node as:

- Bone when S < 1
- Cartilage when 1 < S < 3
- Fibrous connective tissue when S > 3

Values of stimuli over the domain are exported and saved in a file and used in the next iteration. An interpolation function will read the saved file from previous iteration and return the stimuli value based on coordinates. Also, 3 piece wise functions representing Youngs modulus, Poissons ratio and Permeability are defined and use the output of interpolation function to assign the correct material properties to the nodes. The material properties Zhang et al. (1998)Cowin (1999)Kutz (2003)Rémond et al. (2008)Yao et al. (2012) of each node are updated according to Table 1. With the updated material, poroelastic study is ready to be performed again. This procedure is repeated until an equilibrium is reached(Figure 6). An arbitrary iteration is demonstrated in Figure5 and shows the calculated stimuli over the domain(left) and borders(right) separating generated materials to be assigned in next iteration. At the end of this process, solid section of gap is extracted and transferred to the topology optimization module.

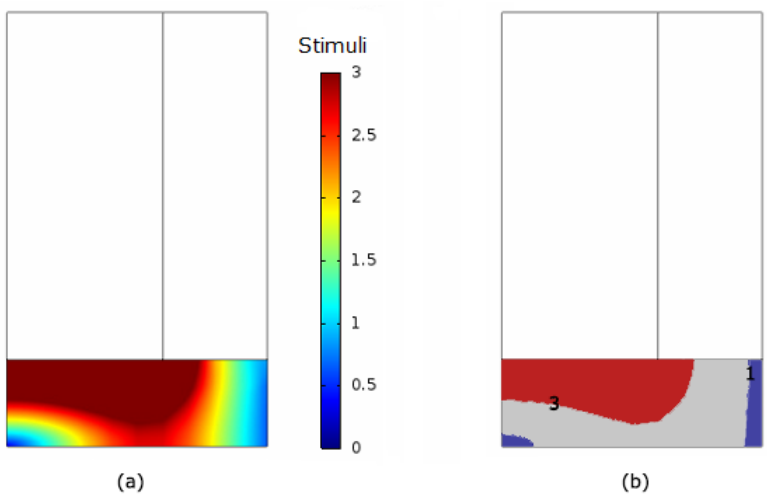

Figure 5: (a) Calculated stimuli and (b) resulting tissues: bone(blue), cartilage(grey) and fibrous connective tissue(red)

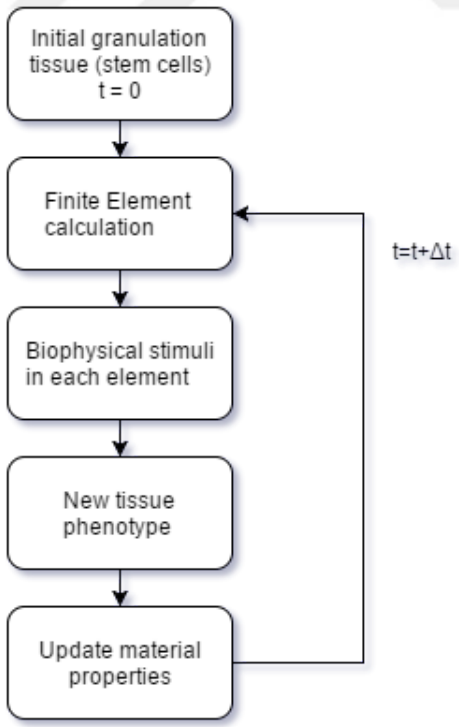

Figure 6: The iterative process regulating tissue differentiation

Table 1: Material properties of tissues

	Young's modulus (Pa)	Poisson's ratio	Permeability (m^2)
Granulation tissue	2e6	0.13	3.5e-17
Fibrous	4e6	0.13	3.5e-17
Marrow	4e6	0.13	3.5e-17
Cartilage	10e6	0.17	3.5e-18
Mature bone	6e9	0.3	1.7e-17
Cortical bone	14e9	0.3	3.5e-20

3.2 Topology Optimization Problem Coupled with Level Set Method

First step to solve the topology optimization problem mentioned in(2.3) is to rewrite the problem in terms of the level set method (Liu et al. (2005)) and build a reaction-diffusion form of equation. To perform topology optimization on an initial 2D structure, Ω. the initial level set function for this domain can be defined as a signed distance function $\phi(x)$:

$$\begin{cases} \phi(x) > 0 & material(x \in \Omega^{+}) \\ \phi(x) = 0 & boundary(x \in \partial\Omega) \\ \phi(x) < 0 & void(x \in \Omega^{-}) \end{cases} \tag{8}$$

where x is a vector defining coordinates of a point in the design domain. Also, a Heaviside function $H(\phi)$ needs to be defined as:

$$H(\phi(x)) = \begin{cases} 1 & \phi > 0 \\ 0 & \phi \leq 0 \end{cases} \tag{9}$$

and its distributional derivative function, Dirac delta $\delta(\phi)$:

$$\delta(\phi(x)) = \frac{\mathrm{d}H(\phi(x))}{\mathrm{d}\phi} \tag{10}$$

Then, elasticity modulus E over the entire design domain can be defined as:

$$E(\phi(x)) = E_0 H(\phi(x)) + E_{min}(1 - H(\phi(x))) \tag{11}$$

where E_0 is the material elasticity modulus and E_{min} is the minimum relative elasticity modulus. Now, the compliance minimization problem, as proposed byLiu et al. (2005) can be written as:

$$\begin{aligned} min \qquad & C(\phi) = \int_\Omega \frac{1}{2} E(\phi)\epsilon^T D\epsilon d\Omega \\ s.t. \qquad & \nabla.(E(\phi)\sigma = f \\ & \int_\Omega H(\phi)d\Omega = Vol^* \end{aligned} \tag{12}$$

Where the design domain is shown by Ω , δ is stress tensor, ϵ is strain tensor, D is the elasticity matrix and Vol^* is the volume limit. In order to make this problem ready to be solved by FEM using level set method, the first constraint will be kept away for now and the objective function will be combined with the second constraint using the Lagrangian formulation. Later, a solid mechanics formulation will solve for strain using the first constraint and plug the solution into the optimization problem to solve for ϕ. This is how the coupling ability of COMSOL is used to solve this problem. Using the Lagrangian multiplier λ we will have:

$$J(\phi, \lambda) = \int_\Omega (\frac{1}{2} E(\phi)\epsilon^T D\epsilon + \lambda(H(\phi) - Vol^*/Vol^\Omega))d\Omega \tag{13}$$

so the variation ϕ on the material boundary will be

$$\begin{aligned} \delta_\phi J &= \int_\Omega (\frac{1}{2}\frac{\partial E(\phi)}{\partial \phi}\epsilon^T D\epsilon + \lambda\frac{\partial H(\phi)}{\partial \phi})\delta\phi|_{\phi=0} d\Omega \\ &= \int_\Omega (\frac{1}{2}\frac{\partial E(\phi)}{\partial \phi}\epsilon^T D\epsilon + \lambda\frac{\partial H(\phi)}{\partial \phi})|\nabla\phi|\delta l d\Omega \\ &= \int_\Omega (\frac{1}{2}(E_0 - E_{min})\epsilon^T D\epsilon + \lambda)\delta(\phi)|\nabla\phi|\delta l d\Omega \end{aligned} \tag{14}$$

giving the corresponding Euler-Lagrange equation at the extreme value, hence we will have

$$\frac{\partial \phi}{\partial t} = (\frac{1}{2}(E_0 - E_{min})\epsilon^T D\epsilon + \lambda)\delta(\phi)|\nabla\phi| = 0 \tag{15}$$

and using gradient projection method proposed by Zhao et al. (1996) λ would be

$$\lambda = -\frac{[\frac{1}{2}(E_0 - E_{min})\epsilon^T D\epsilon])\delta^2(\phi)|\nabla\phi|d\Omega}{\int_\Omega \delta^2(\phi)|\nabla\phi|d\Omega} \tag{16}$$

Now in COMSOL, two studies are defined, one solving for the stress and strain 2, and the other one solving the reaction-diffusion equation for ϕ as:

$$\frac{\partial\phi}{\partial t} - [\frac{1}{2}(E_0 - E_{min})\epsilon^T D\epsilon + \lambda]\delta(\phi)|\nabla\phi| = \alpha\triangle\phi \tag{17}$$

Even though it was assumed that the volume constraint is going to be satisfied throughout the optimization process, use of numerical methods to calculate the constraint value will inherently introduce a small computational non-zero error. Because of this error, the area constraint may not be satisfied in all the iterations. To overcome this problem, a penalty term is added to the volume constraint.

$$PenaltyTerm = \beta(lm_area - Vol*) \tag{18}$$

where β is the penalty factor, lm_area is the area calculated in each iteration.

Before defining the studies in COMSOL, some numerical functions are implemented as well. First of all, a compactly supported radial basis function is defined to track the velocity field in a controlled bandwidth of material boundary.

$$f_{rbf} = (1 - r)_+^{12} \tag{19}$$

Also, to control the slope of level-set function and to speed up the convergence, $|\nabla\phi|$ is replaced by $min(gradmax, |\nabla\phi|)$ where $gradmax$is a suitable constant.

Finally, to smooth the strain energy($\epsilon^T D\epsilon$) function. initial value of strain energy $Strainmax$ is calculated based on the initial ϕ and then the strain energy function($\epsilon^T D\epsilon$) is replaced by $min(Strainmax, \epsilon^T D\epsilon)$

For the first part, a "Solid Mechanics" model and a "Steady State" study was chosen. Figure 7 shows the implementation in COMSOL. Geometry and boundary conditions are shown in Figure 8.

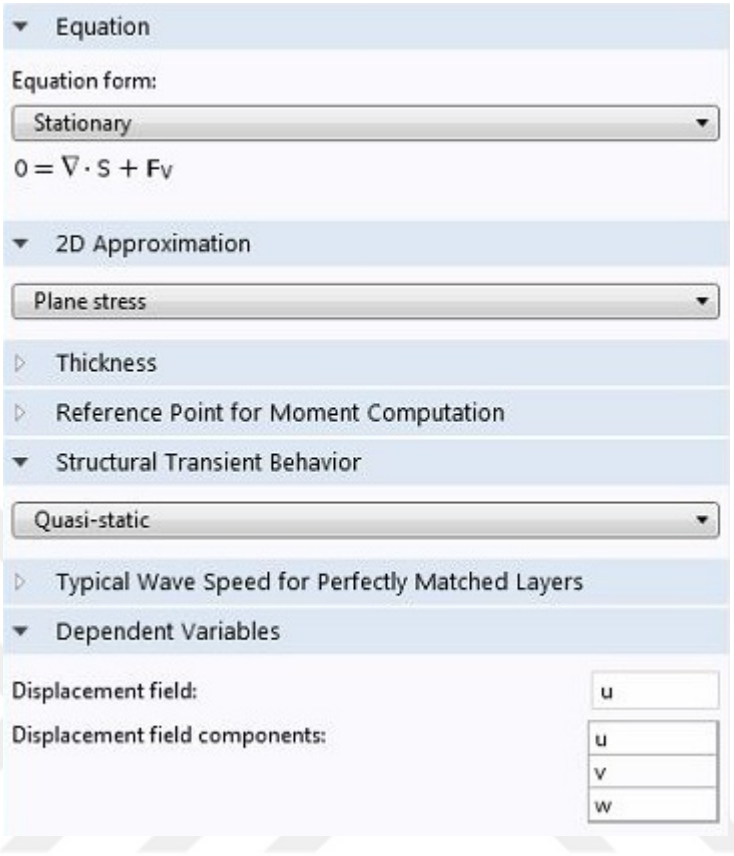

Figure 7: Solid mechanics equation in COMSOL

Next, to simulate the second study, a ”General Form PDE” model and a ”Time Dependent” solver is created. Then, Equations 9 and 10 are defined using the built-in step function of COMSOL and an analytic function computing its derivative. Also, a radial basis function is set as in Equation 19. For this module, the coefficients of Equation 17 will be inserted as shown in Figure 9.

Cooperation of these two studies is controlled with MATLAB, where we can define a loop and pass the solutions between studies. The algorithm behind the MATLAB code is demonstrated in Figure10.

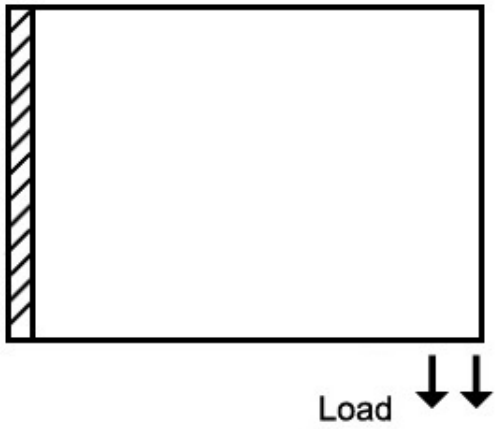

Figure 8: Boundary conditions of topology optimization problem where left end is fixed and load is applied at 1/16 length of lower boundary

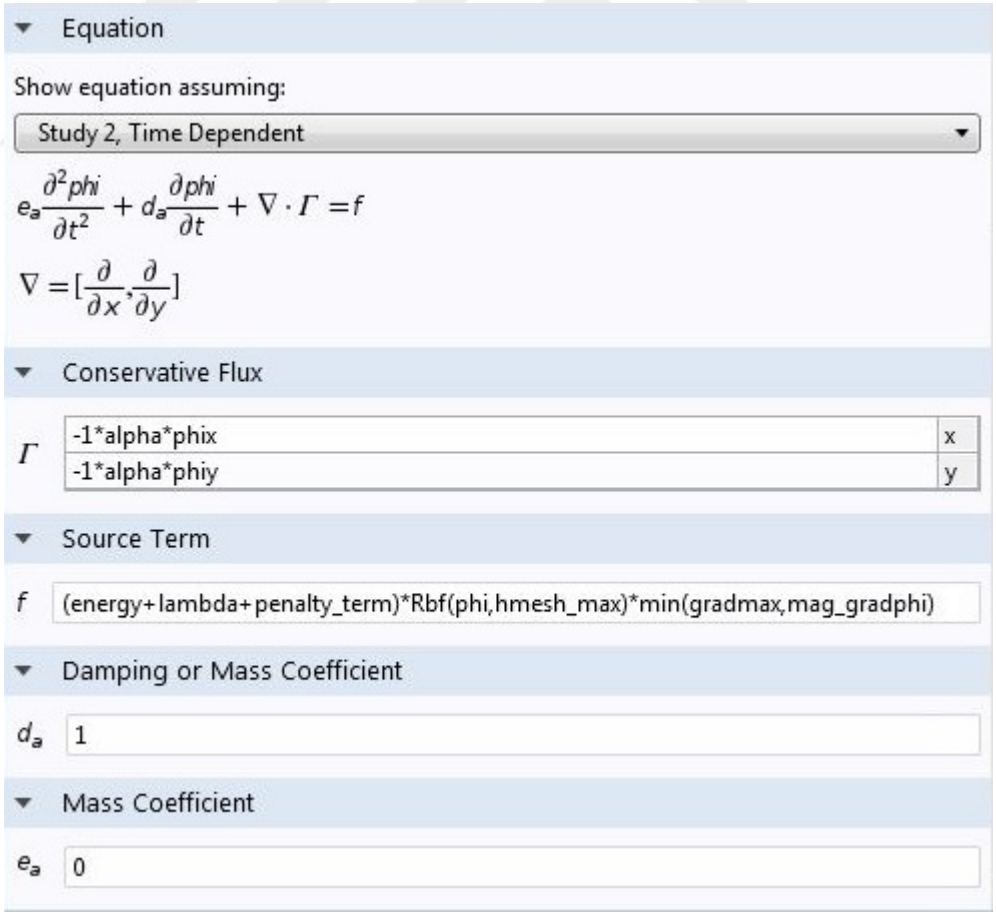

Figure 9: PDE equation in COMSOL

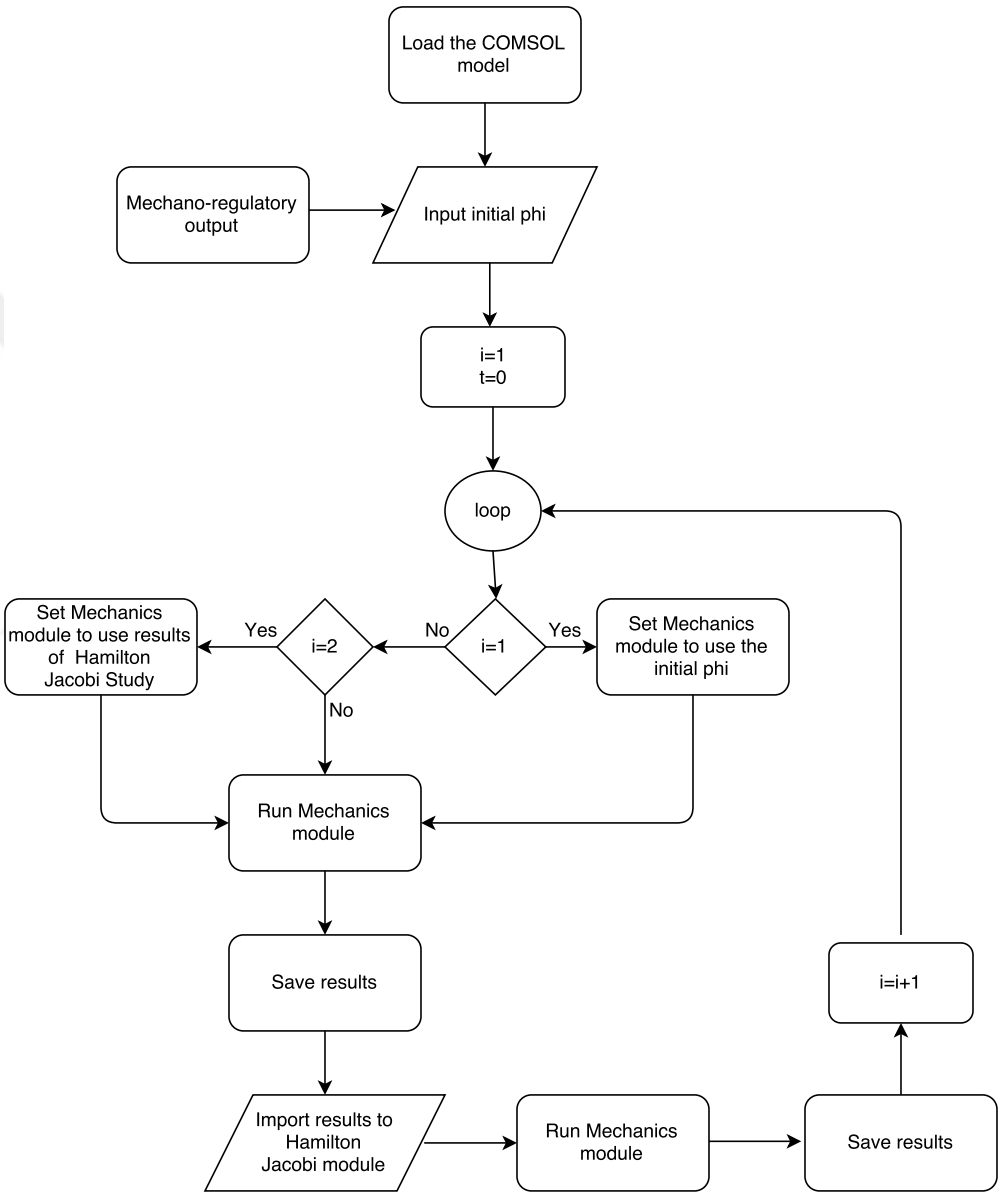

Figure 10: Topology optimization flowchart

4 Results

4.1 Mechano-regulatory Model

The mechano-regulatory algorithm explained in Section 3.1 has been applied to the 10mm gap model(Figure4) in a poroelastic setting using COMSOL Multiphysics. In this thesis, bone is considered as an isotropic linear material. Marrow canal has a radius of 9mm and outer radius of cortical bone is 15mm. Biot-Willis coefficient is set to 0.2 and porosity of 0.8 is approximated for all the tissues. As expected and was proven in Lacroix et al. (2002) all the stem cells in gap differentiate to bone in 8 iterations. Figure11 shows the average modulus of elasticity in gap throughout the study. Calculated stimuli and resulting tissue evolution are obtained as in Figure 12 and Figure 13, respectively. The obtained bone tissues will be used later in (Section 4.3) as an initial structure in the topology optimization model.

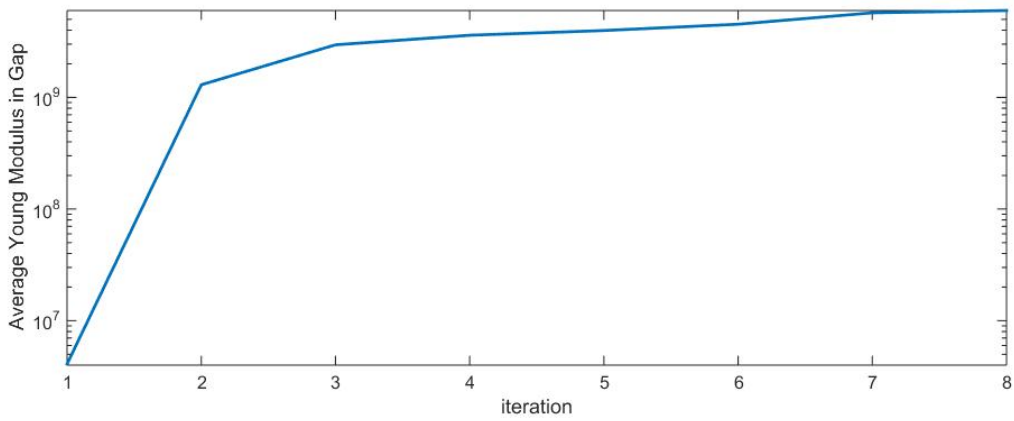

Figure 11: Average modulus of elasticity obtained in the gap of the broken bone model of Figure 4 via mechano-regulatory model in iterations 1 to 8

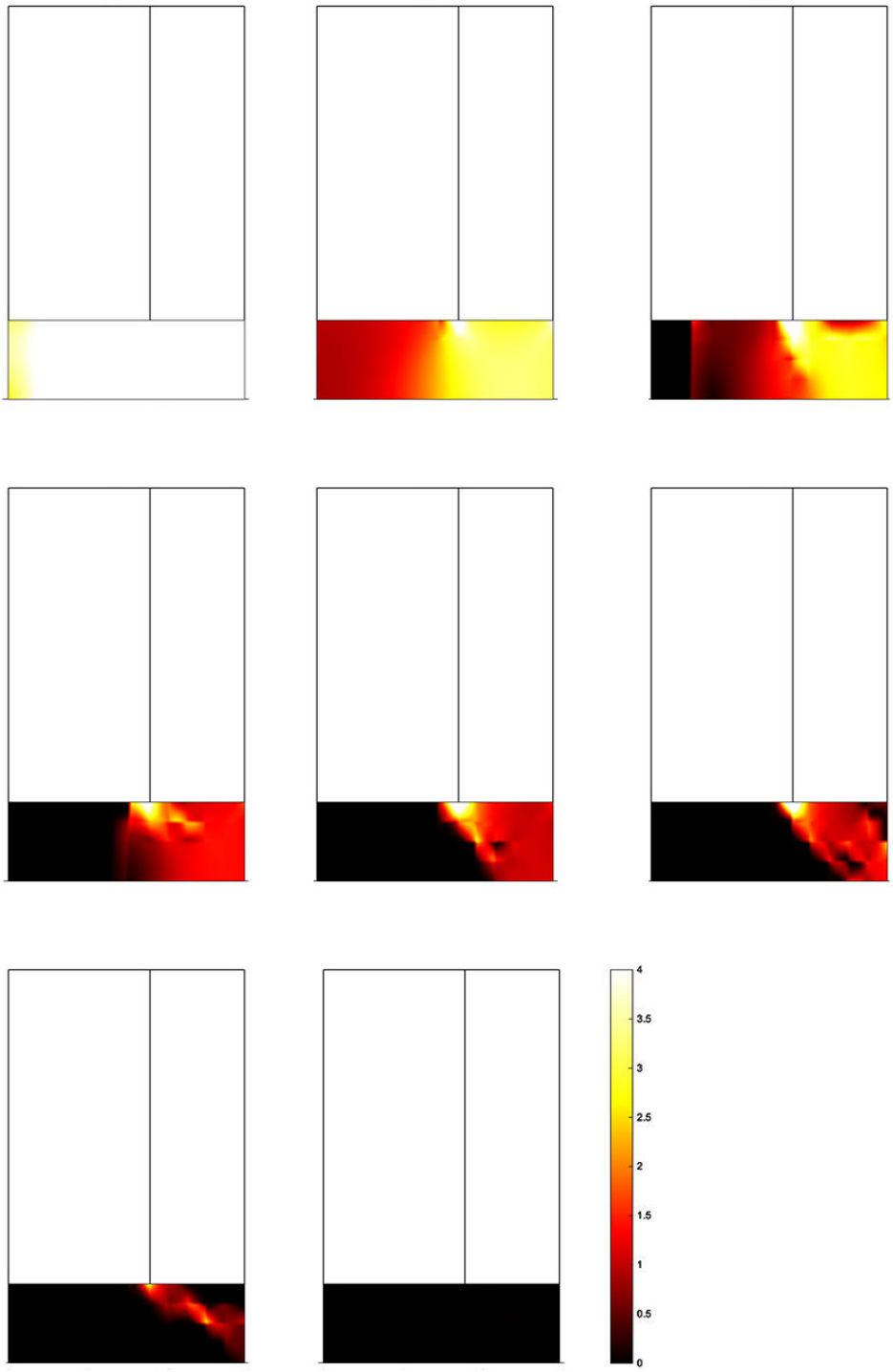

Figure 12: Calculated stimuli obtained in the gap of the broken bone model of Figure 4 via mechano-regulatory model in iterations 1 to 8

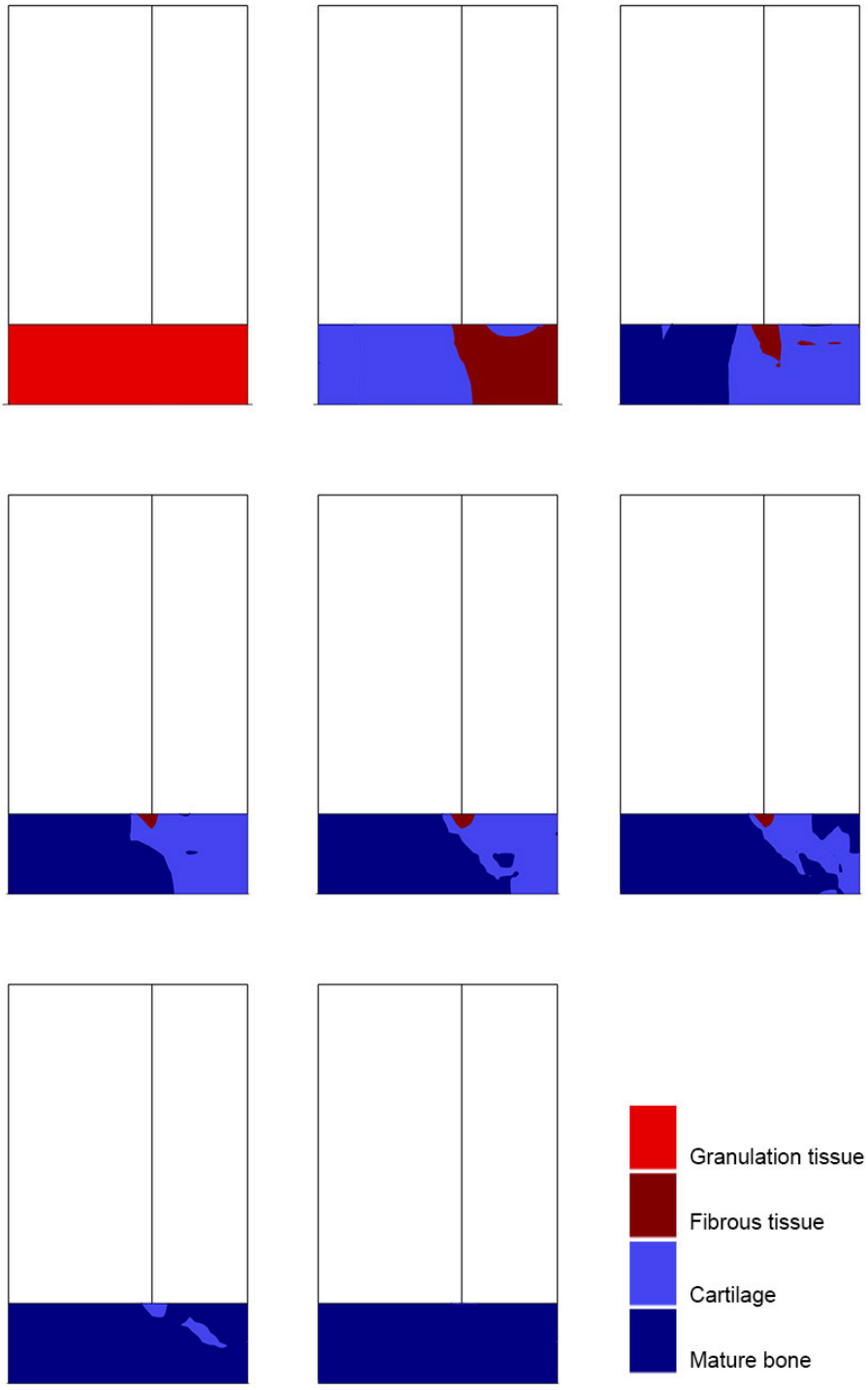

Figure 13: Generated tissues types obtained in the gap of the broken bone model of Figure 4 via mechano-regulatory model in iterations 1 to 8

4.2 Topology Optimization on the 2D Cantilever Beam Benchmark Problem

The topology optimization model based on the level set method as described in Section 3.2 has been applied to the benchmark problem of a cantilever beam as done by Liu et al. (2005). The final strain energy shows 1.7% difference from the value of the result in Liu et al. (2005). Figure14 shows the corresponding change in topology from initial value to the optimal one. Also, Figure15 depicts the convergence history of the minimized strain energy, the gradient descent flow and the area constraint error of the optimization process. When compared with the benchmark problem results, these are in agreement and validate the developed topology optimization framework. Model's reaction to changing certain parameters such as mesh size, mesh type, initial level set and volume constant is examined through five more studies. Table 2 summarizes parameters used in each of these studies and their convergence time.

Table 2: Parameters used in different studies on cantilever beam

Study Number	Vol* Percentage	Radius of Initial Cavities(R)	Number of Elements(N)	Mesh Type	Time [s]
1	50	0.8	3039	Free Trigular	645
2	50	0.2	3039	Free Trigular	1202
3	40	0.8	3039	Free Trigular	483
4	70	0.8	3039	Free Trigular	989
5	50	0.8	5424	Free Triangle	868
6	50	0.8	5312	Free Quadrilateral	921

Comparing studies 1 and 2 indicates that the the final solution is almost independent of initial level-set. However, a smaller area constraint error in the beginning of the process assists a faster convergence. Studies 3 and 4 proves that the volume percentage of final topology can be defined by user. This is a very powerful feature giving many options to be considered while designing an optimal structure. Study 5 compared to study 1 implies that higher precision in mesh, prolongs the computation time as expected but does not have any other significant effect on the optimization result. Study 6 shows that a quadrilateral mesh is also suitable for this problem.

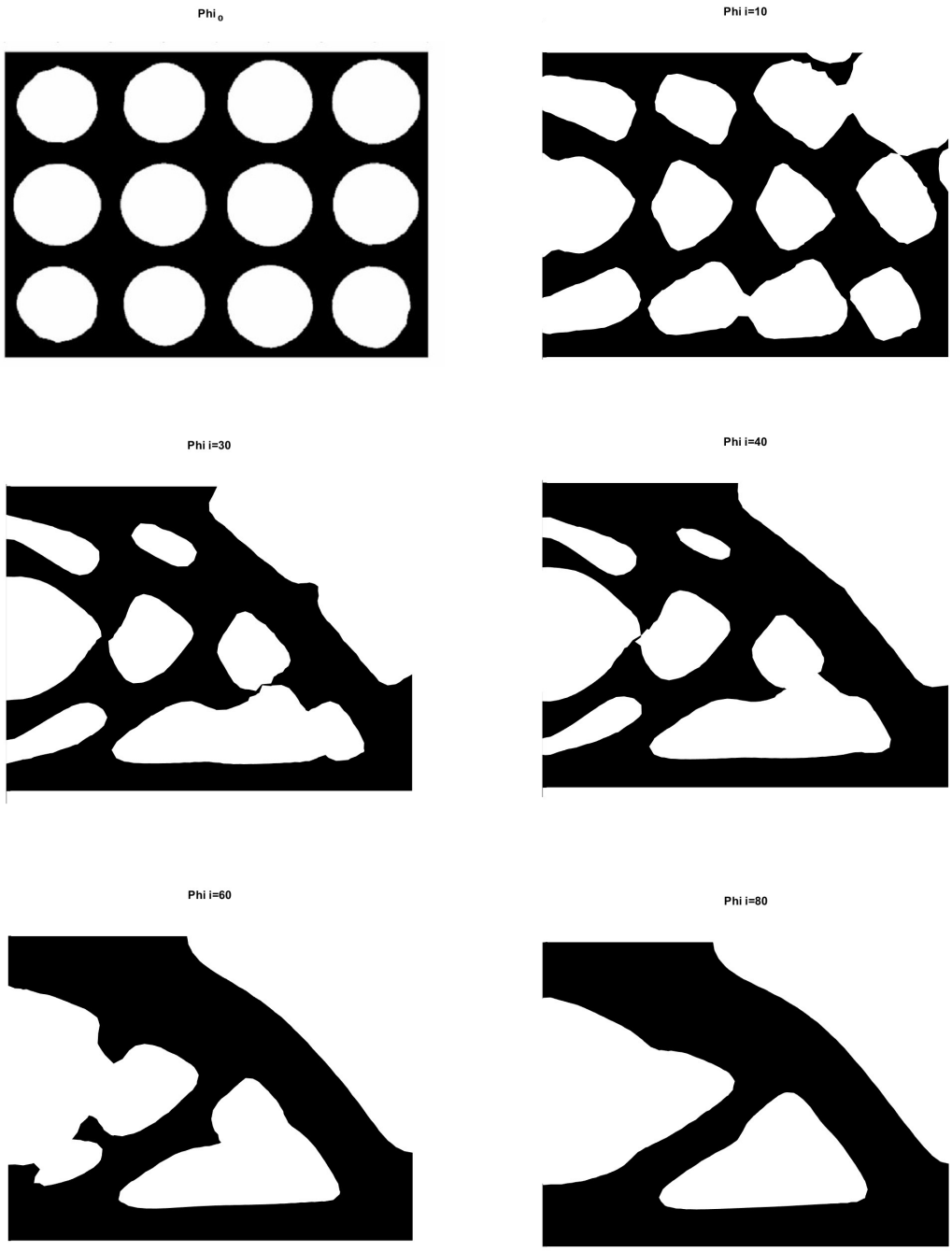

Figure 14: Evolution of ϕ from the initial value in study 1 where Vol^* =0.5, R=0.8, N=3039 and mesh is triangular

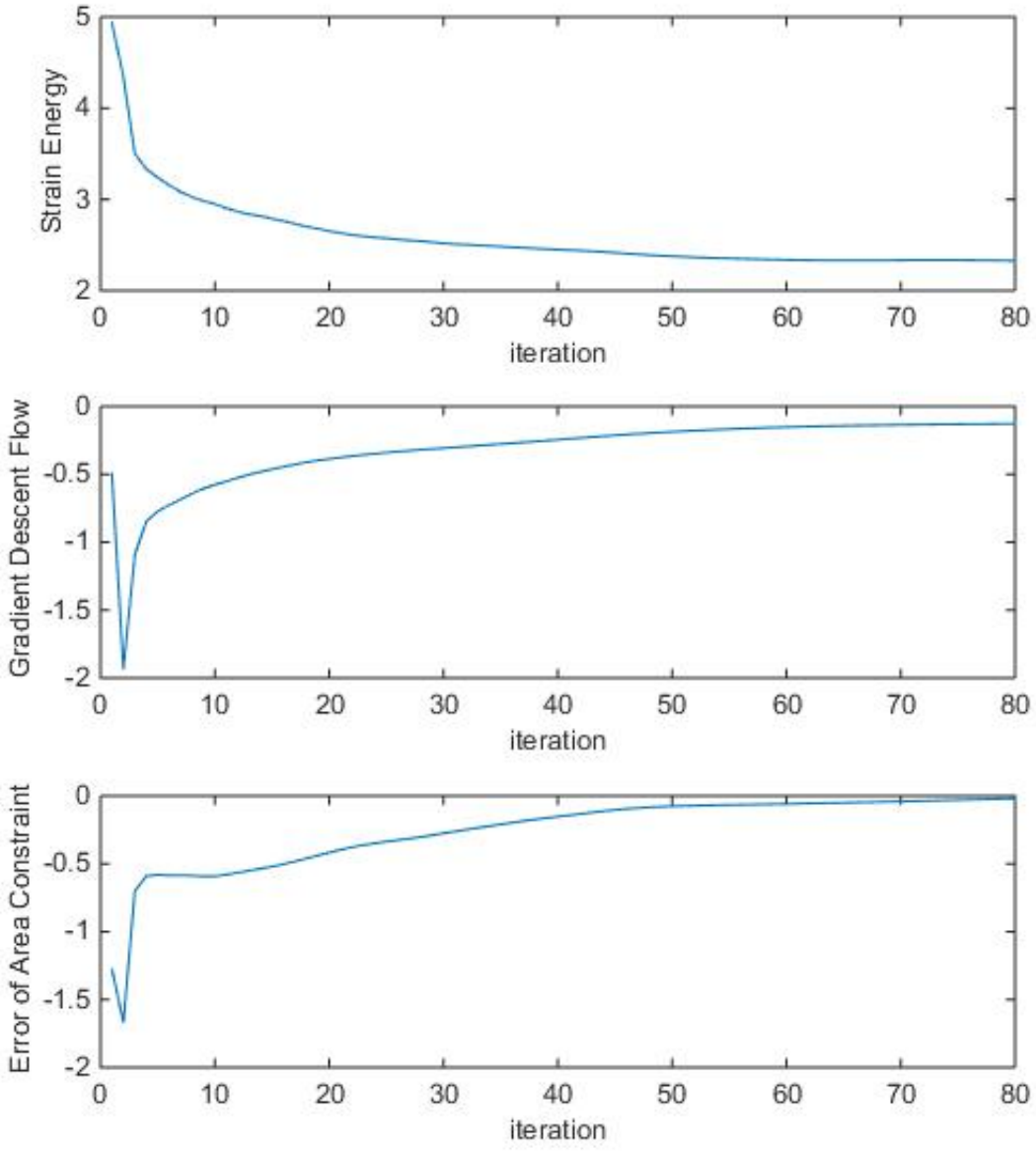

Figure 15: Evolution of ϕ from the initial value in study 1 where Vol^* =0.5, R=0.8, N=3039 and mesh is triangular

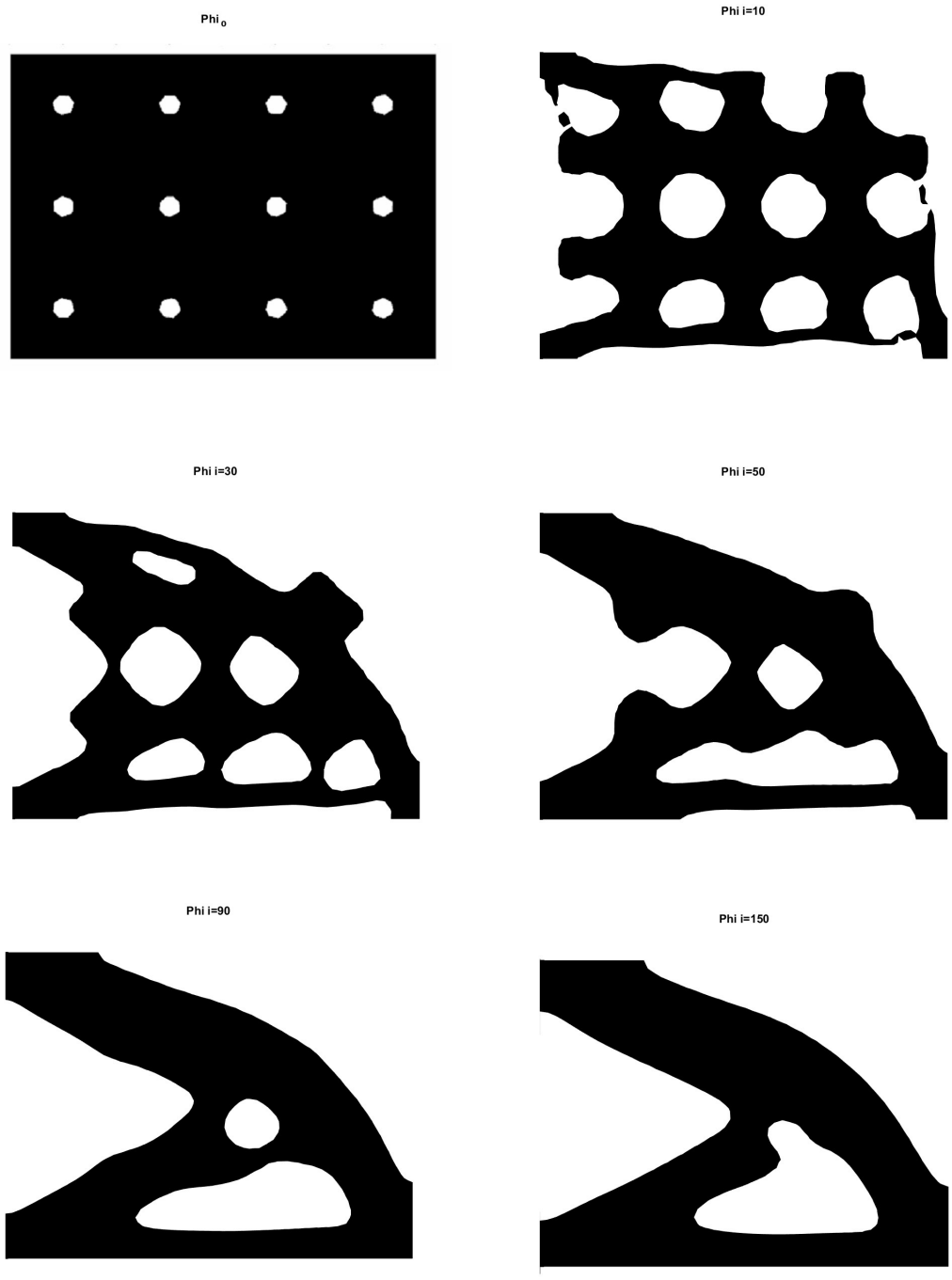

Figure 16: Evolution of ϕ from the initial value in study 2 where Vol^* =0.5, R=0.2, N=3039 and mesh is triangular

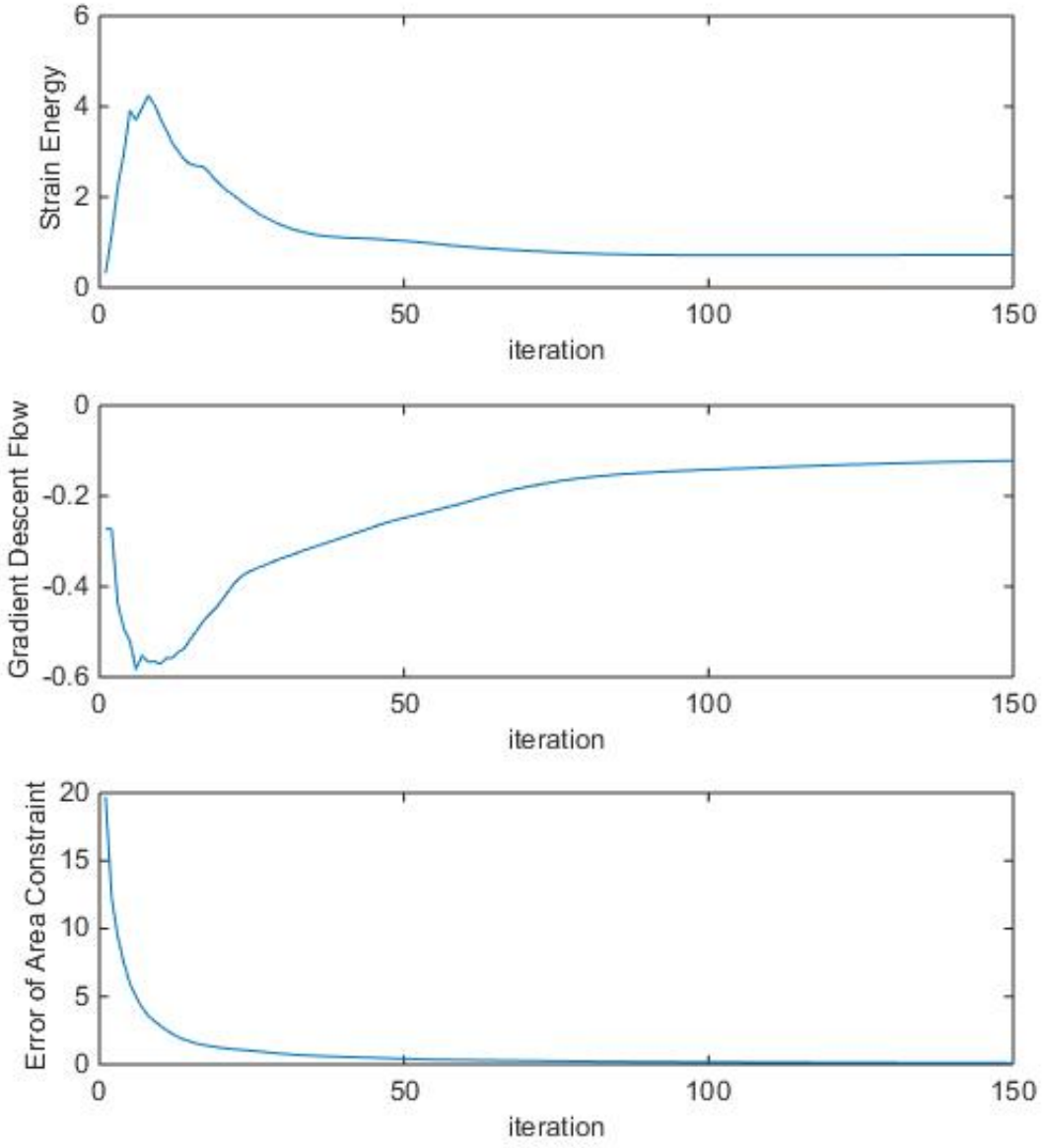

Figure 17: Performance of optimization procedure on cantilever beam in study 2 where Vol^* =0.5, R=0.2, N=3039 and mesh is triangular

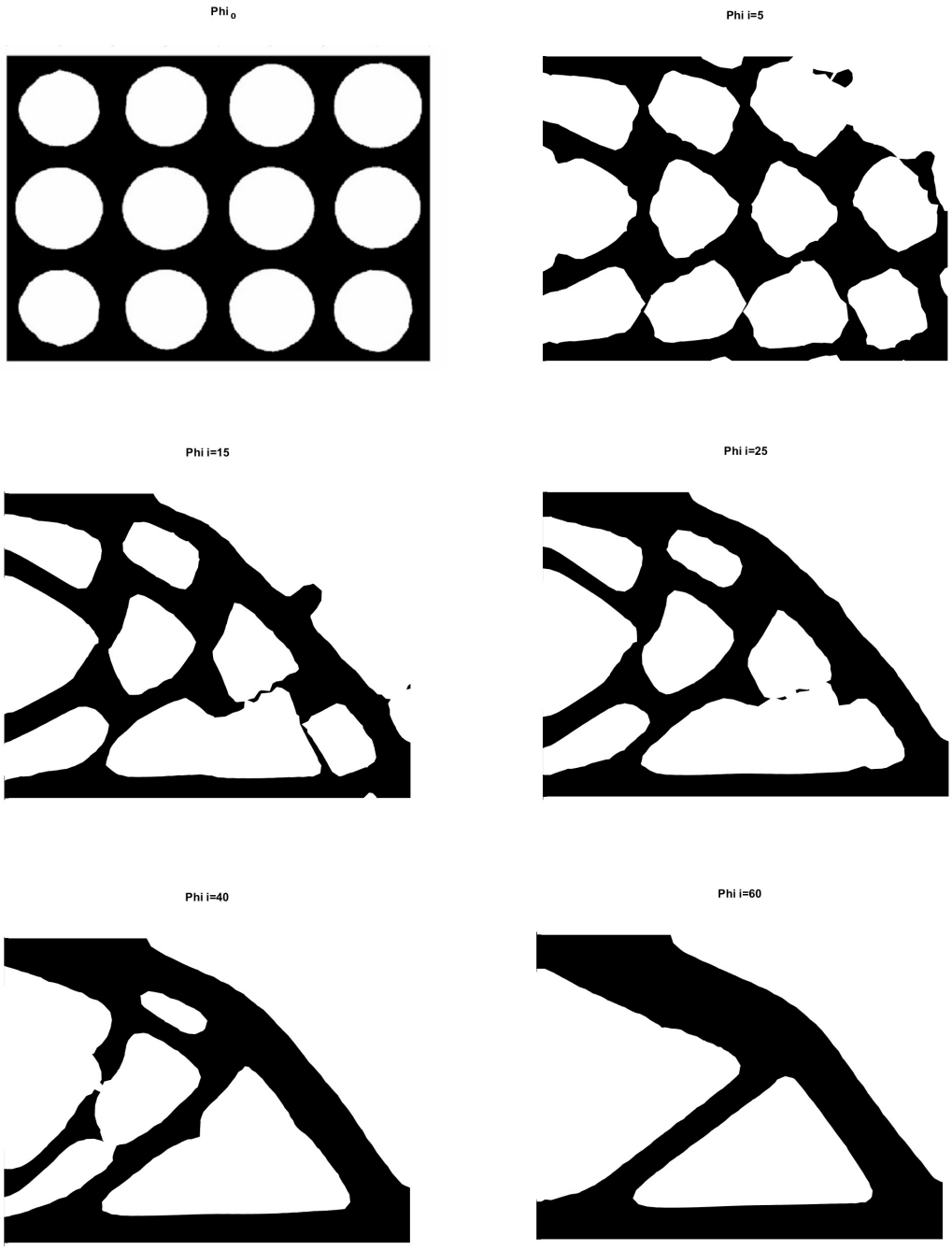

Figure 18: Evolution of ϕ from the initial value in study 3 where Vol^* =0.4, R=0.8, N=3039 and mesh is triangular

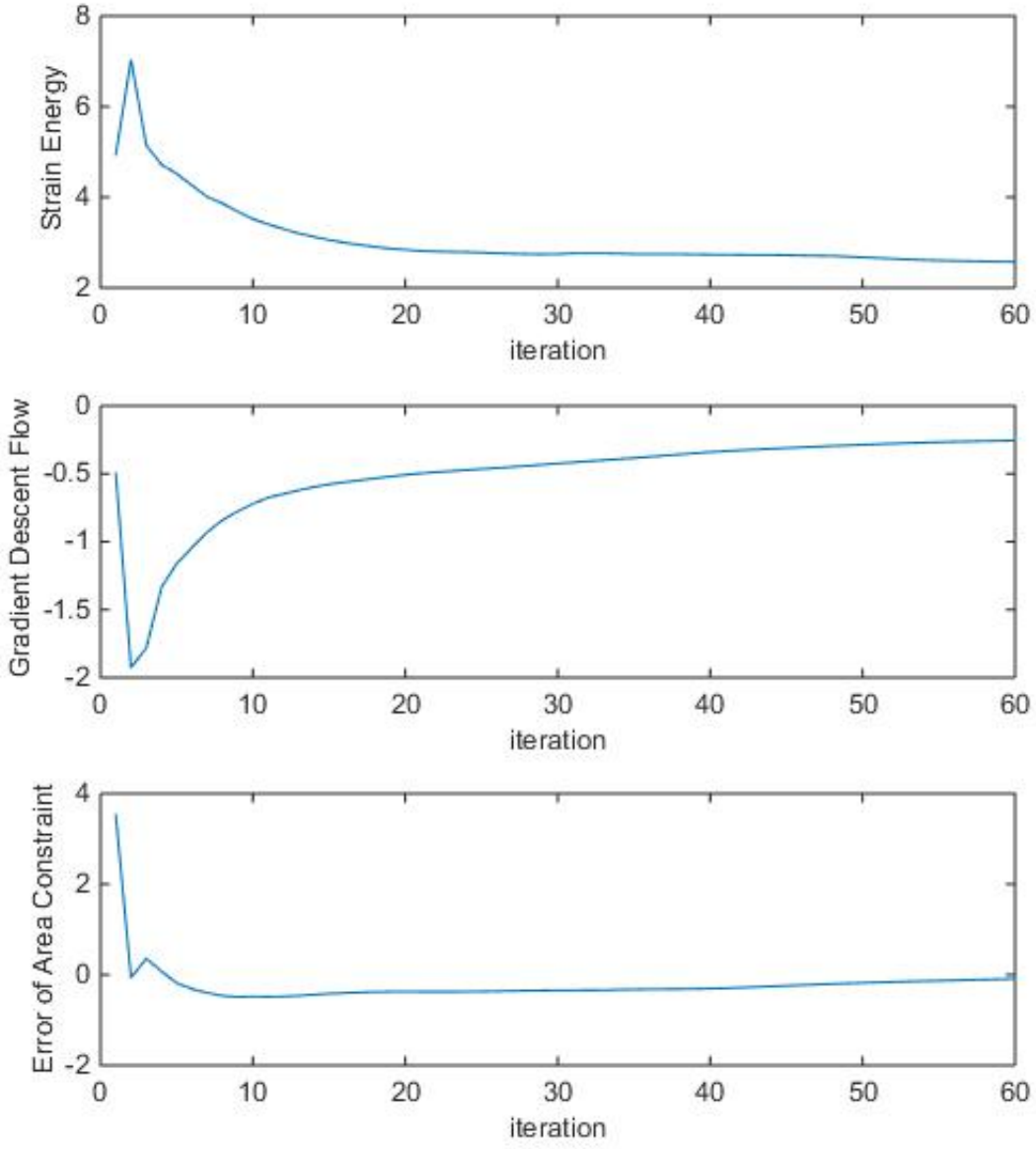

Figure 19: Performance of optimization procedure on cantilever beam in study 3 where Vol^* =0.4, R=0.8, N=3039 and mesh is triangular

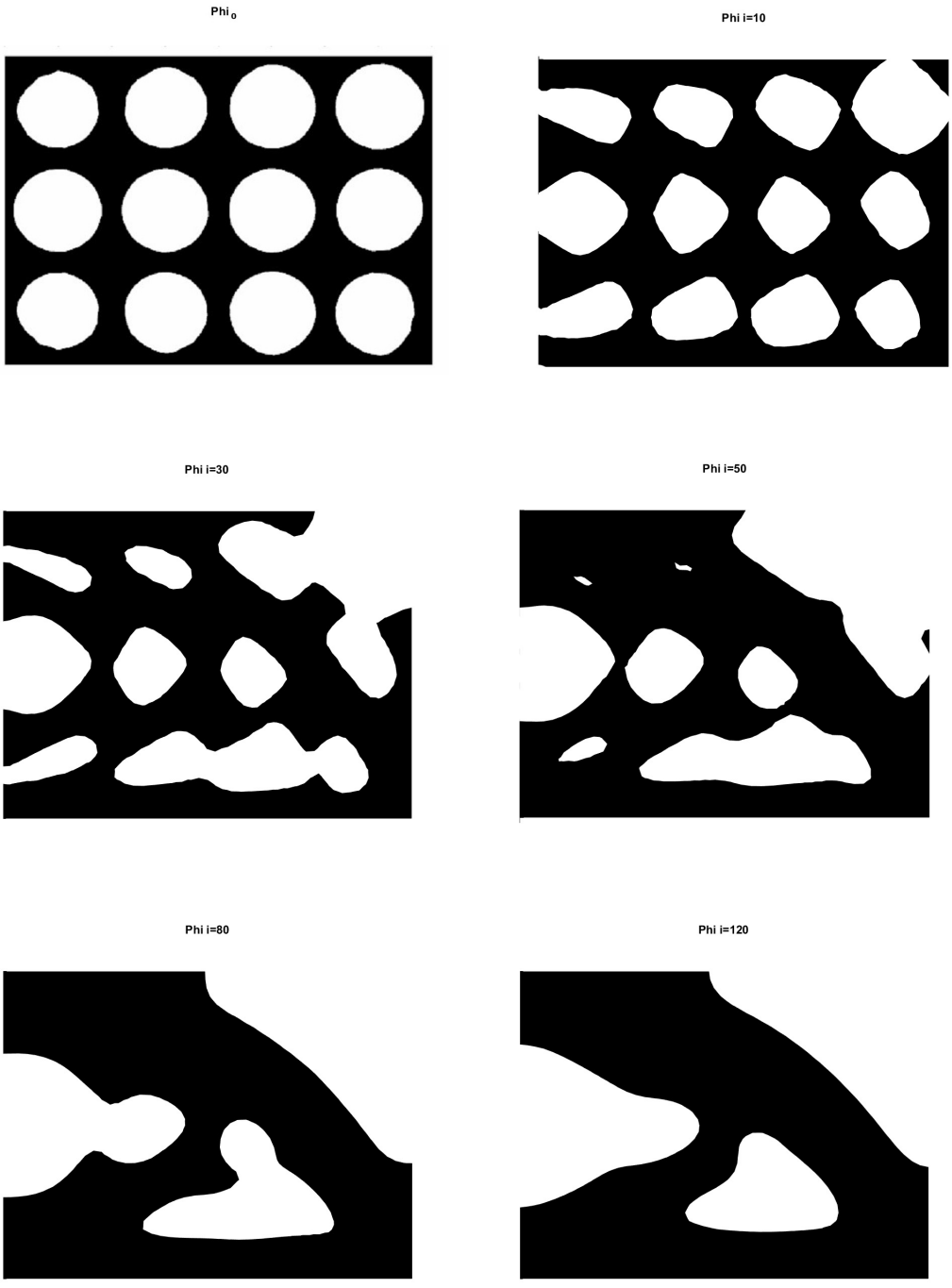

Figure 20: Evolution of ϕ from the initial value in study 4 where Vol^* =0.7, R=0.8, N=3039 and mesh is triangular

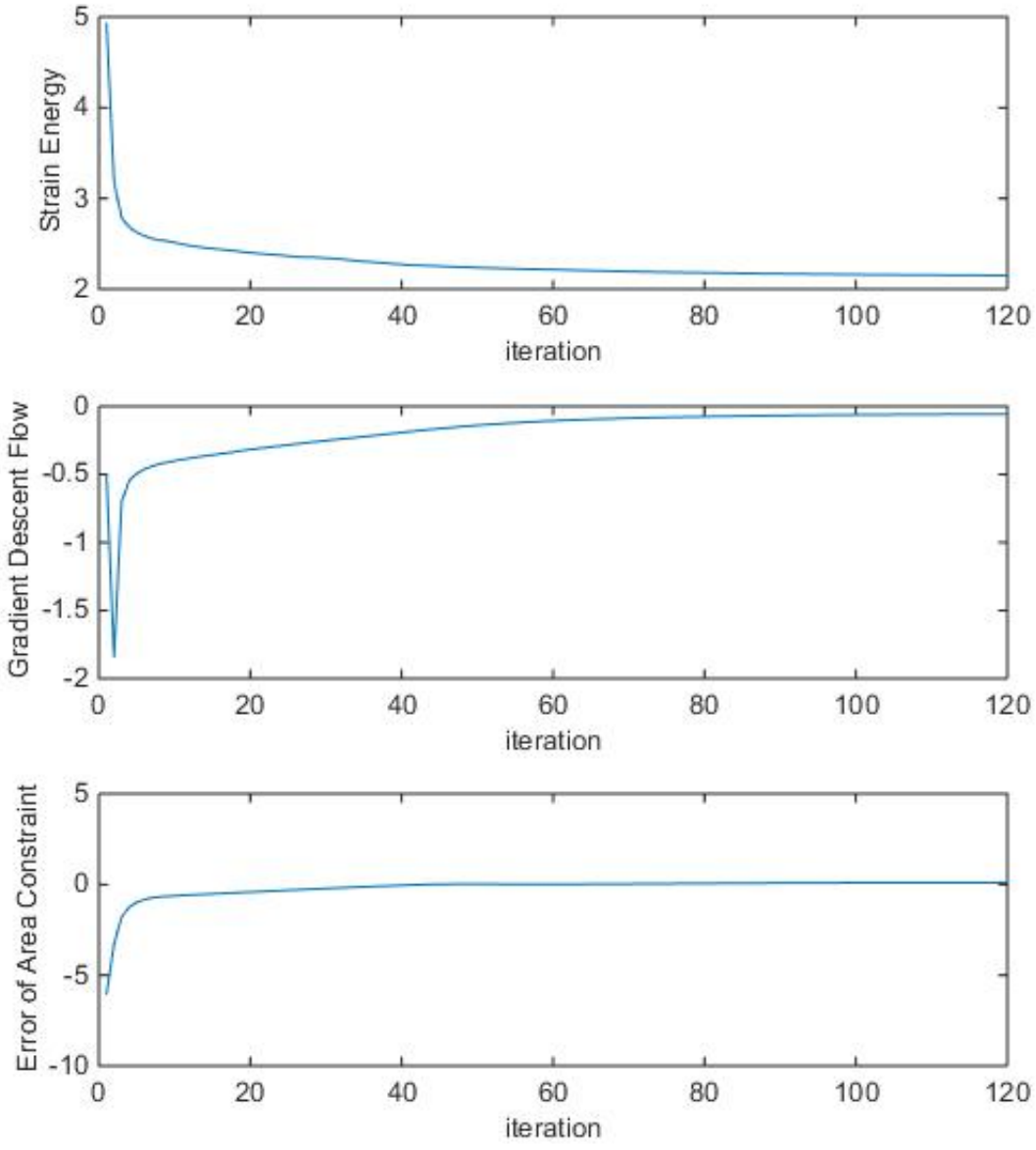

Figure 21: Performance of optimization procedure on cantilever beam in study 4 where Vol^* =0.7, R=0.8, N=3039 and mesh is triangular

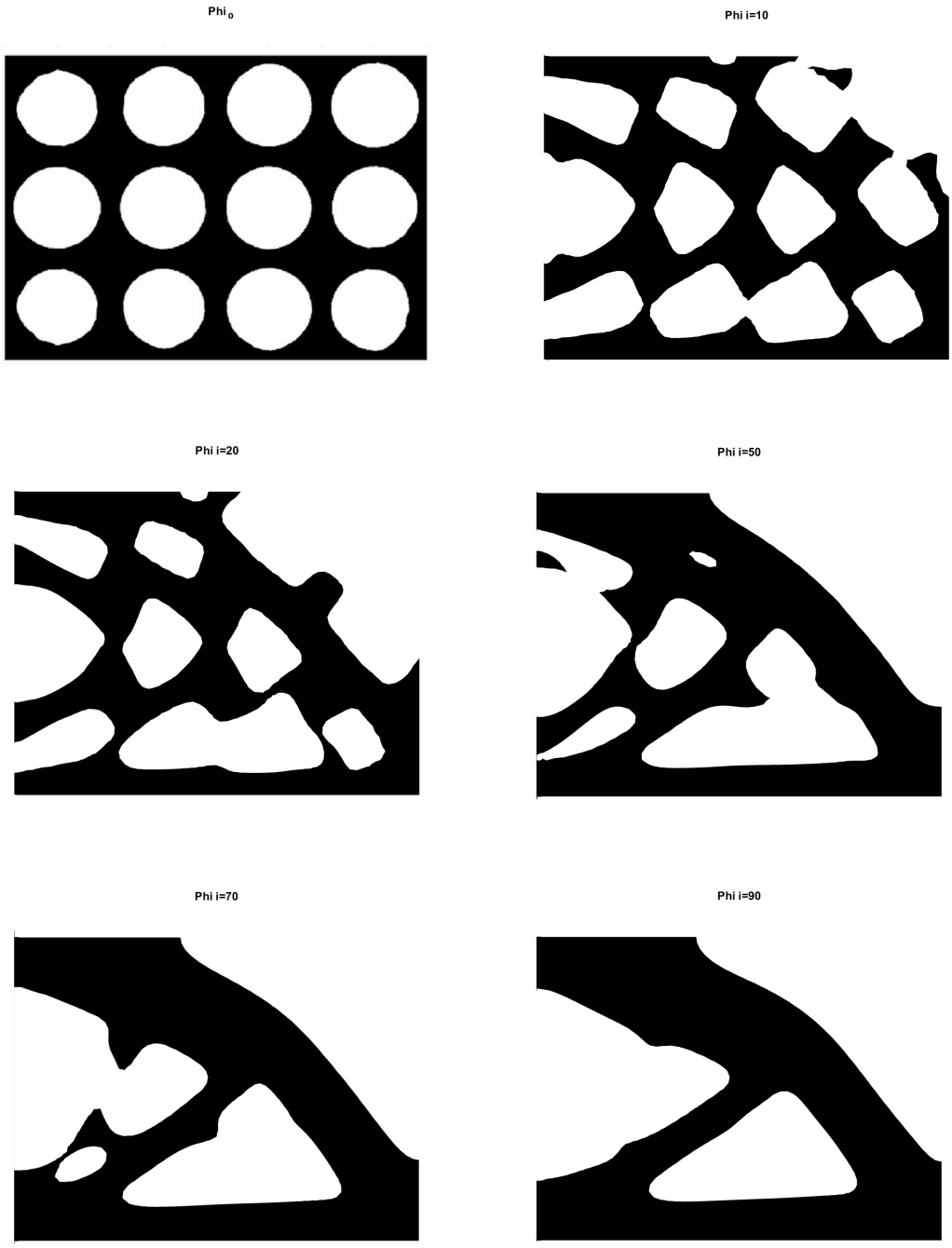

Figure 22: Evolution of ϕ from the initial value in study 5 where Vol^* =0.5, R=0.8, N=5424 and mesh is triangular

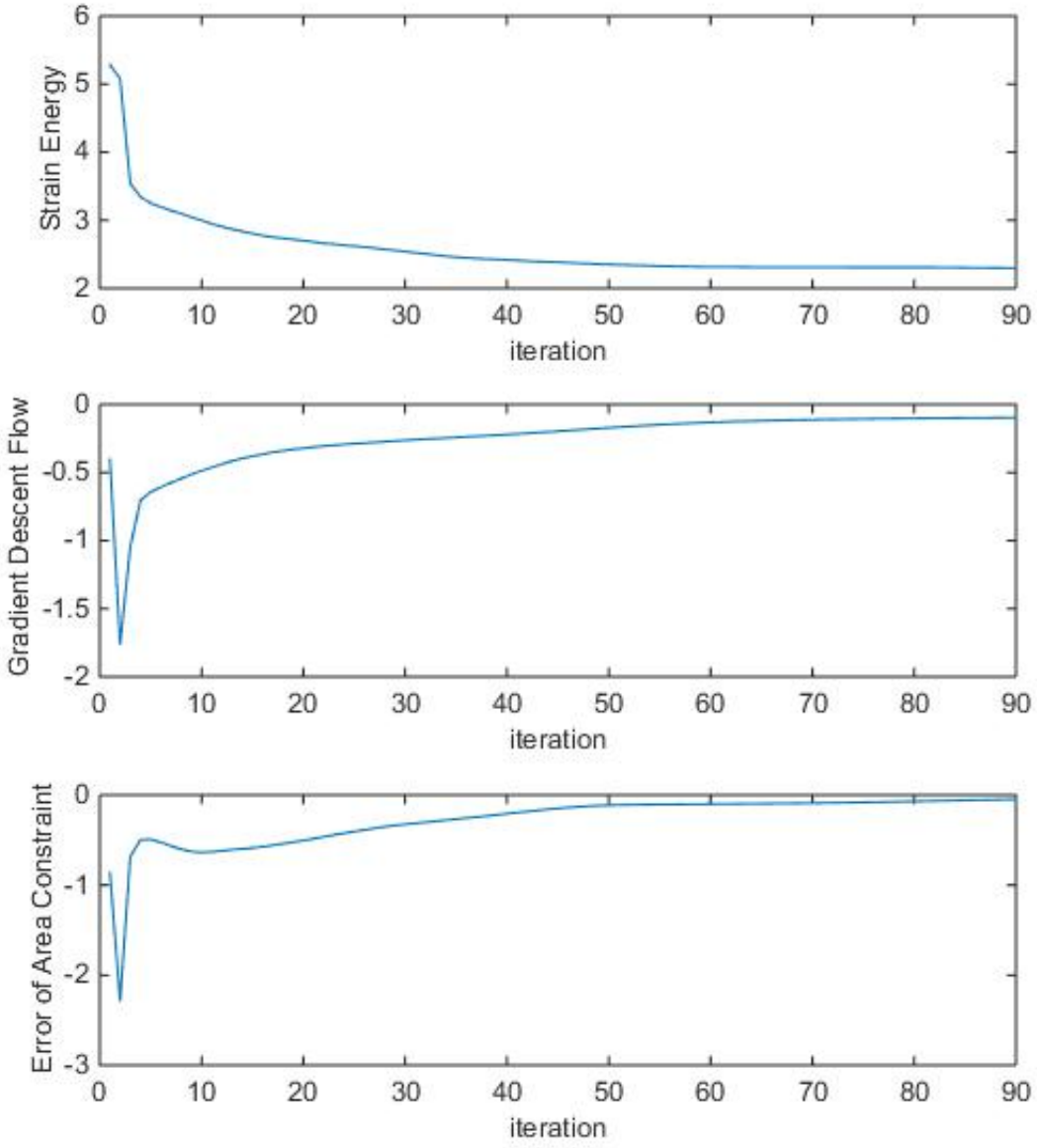

Figure 23: Performance of optimization procedure on cantilever beam in study 5 where Vol^* =0.5, R=0.8, N=5424 and mesh is triangular

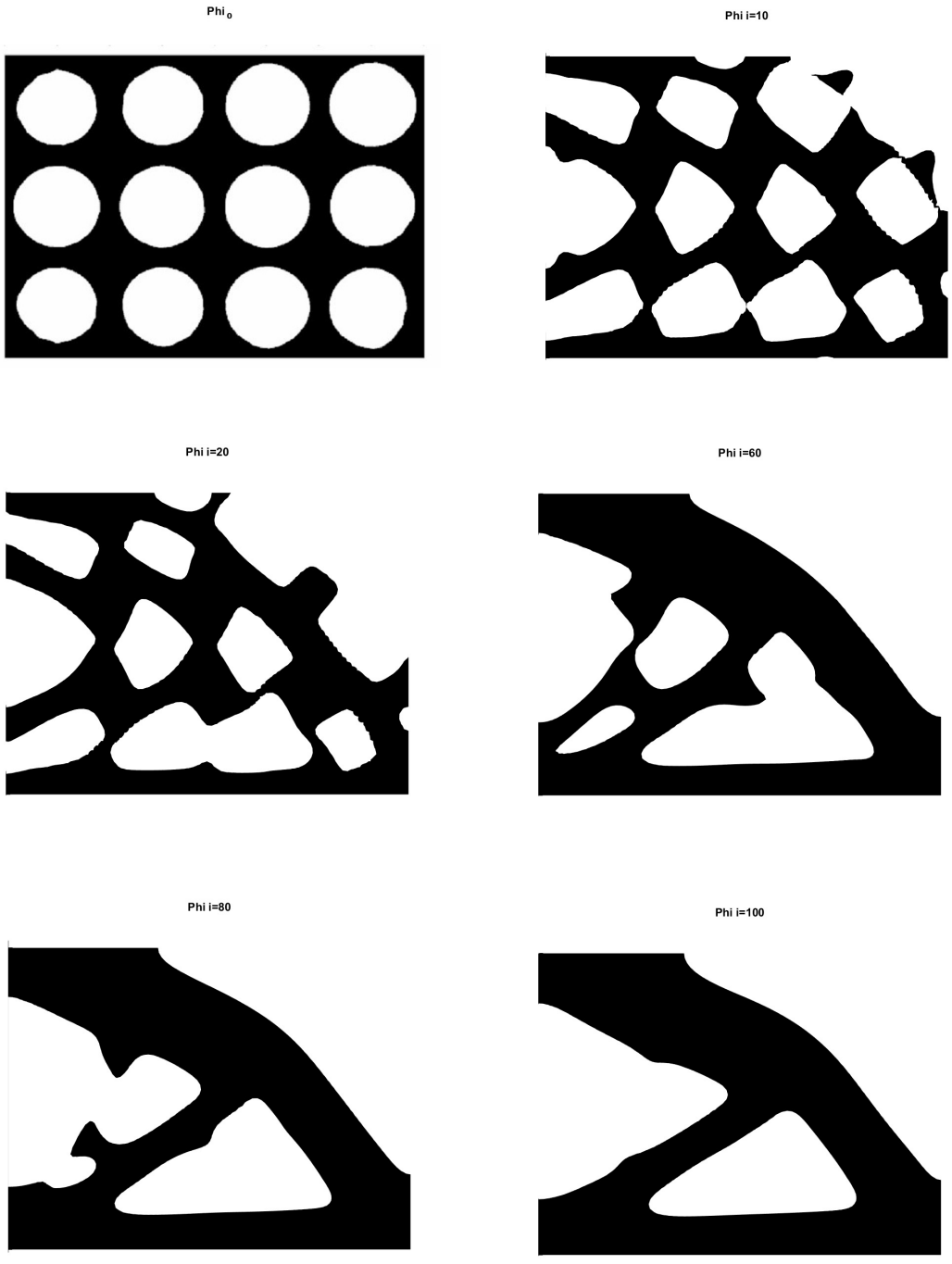

Figure 24: Evolution of ϕ from the initial value in study 6 where Vol^* =0.5, R=0.8, N=5312 and mesh is quadrilateral

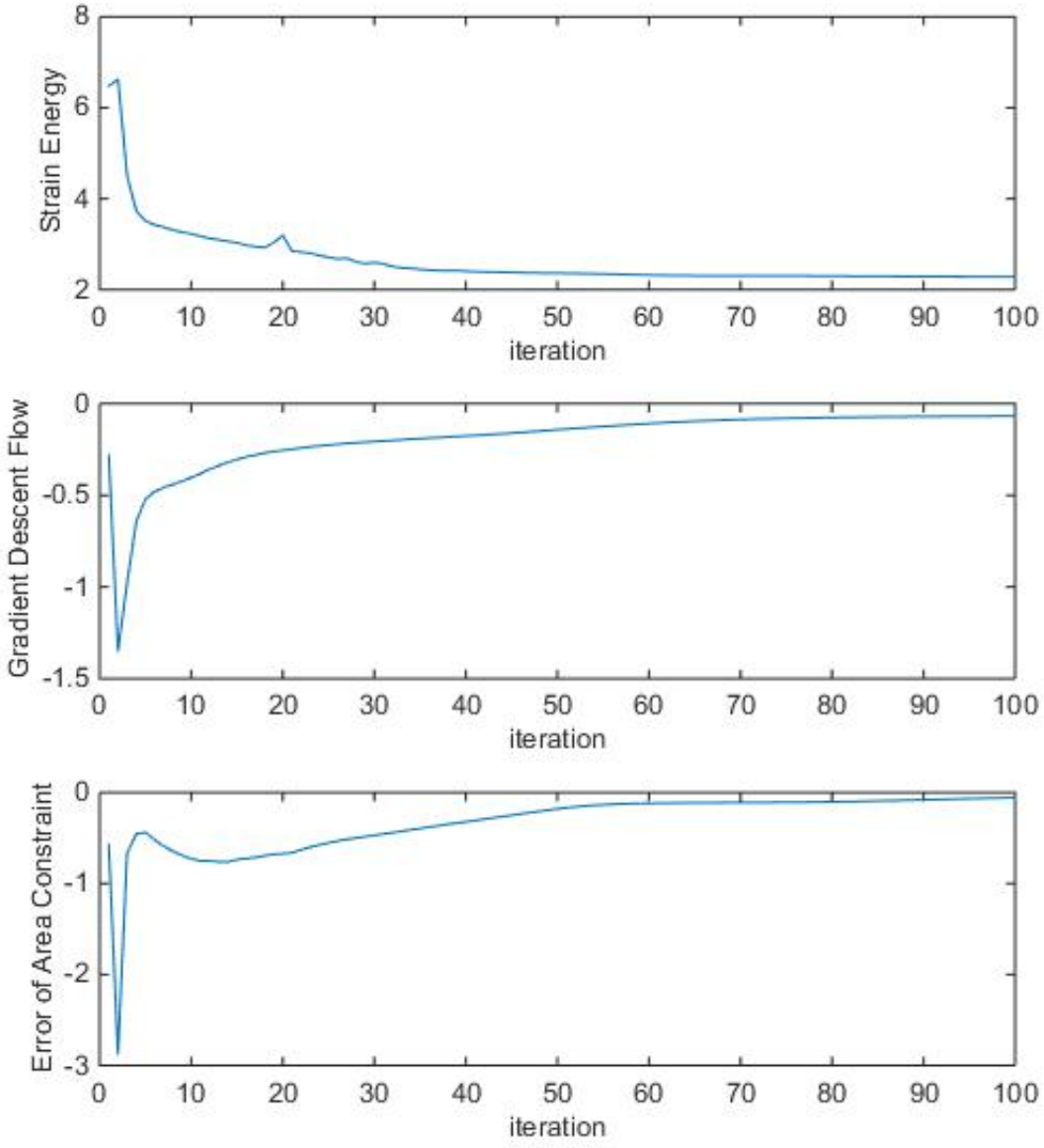

Figure 25: Performance of optimization procedure on cantilever beam in study 6 where Vol^* =0.5, R=0.8, N=5312 and mesh is quadrilateral

4.3 Integrated Design Result for a Topology Optimized Bone Formation in a Fracture Gap Based on Mechanoregulatory Model

The same topology optimization algorithm used in Section4.2 is applied in this section on the solid structure of bone formed in a fracture gap as a result of the mechano-regulatory model as discussed in Section4.1 considering three different sets of boundary conditions(Figure26). Results obtained for each design case with different boundary conditions are shown in terms of the updated level set surface and corresponding convergence histories for strain energy, descent flow and error of the volume constraint, respectively. The first study with the first case of boundary conditions where entire lower bottom surface is supported (Figure26(a)) delivered results in Figure 27 and Figure 28 with a desired volume set to 70%. In the following cases, namely case 2, boundary condition is changed from totally constrained bottom to only 3/5 of of it(adjusted with cortical bone) being constrained as shown in Figure 26(b), in order to create an opening similar to the medullary cavity that exist in natural bones. The second case is used in studies 2 delivered results in Figure 29 and Figure 30 with a desired volume set to 70% and in study 3 delivered results in Figure 31 and Figure 32 with a desired volume set to 60%. In the third case, boundary conditions are adjusted so as to mimic the full axisymmetric profile of the bone scaffold. Figure 33 and Figure 34 show optimization results on a 60% volume constrained model with a penalty parameter $\beta = 10^{-3}$. Figure 35 and Figure 36 show optimization results on a 60% volume constrained model with penalty factor $\beta = 5 * 10^{-3}$. Table 3 summarizes boundary conditions, volume fractions and β parameters used in each of these studies.

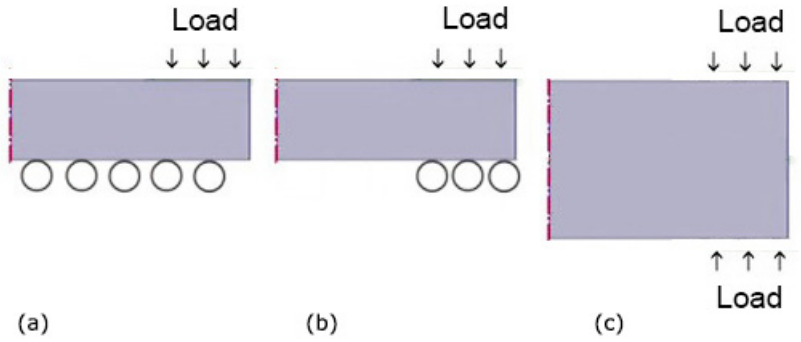

Figure 26: First(a), second(b) and third(c) cases of boundary conditions

Table 3: Boundary conditions and parameters used in different studies on bone formation in fracture gap

Study Number	Boundary Condition Case Number	Vol* Percentage	Penalty Term β
1	1	0.7	10^{-3}
2	2	0.7	10^{-3}
3	2	0.6	10^{-3}
4	3	0.6	10^{-3}
5	3	0.6	$5*10^{-3}$

Figure 28 shows that even though strain energy is increasing at the beginning of study 1, topology is finally optimized going down from a strain energy value of 2e-4 to 2e-8. Second set of boundaries as shown in Figures 29-32 derive more convenient structure by removing the barrier in marrow canal and also reducing the value of strain energy dramatically. When compared with earlier two cases, as evident in Figure 33, the design case with the third boundary condition seems to perform best, given the reduction in the strain energy convergence curve and the resulting optimal topology in Figure 34 despite the unstable convergence curve of gradient descent flow indicating non-smooth disconnected boundaries of the corresponding topologies during the optimization process. This behavior seems to stabilize at the end of the optimization process with a smoother and connected outer boundary obtained for the resulting topology in Figure 34. However, similar to other two design cases, this final design does not satisfy the desired volume constraint. To overcome this issue, the penalty parameter beta is increased from 10^{-3} to $5 * 10^{-3}$ and an additional design study is performed with exact same settings of design case 3 resulting in the level set function change as shown in Figure 35 and convergence history graphs shown in Figure 36. As expected, this parametric change results in the satisfaction of the volume constrained as evident from the volume constraint error convergence graph in Figure 36 converging to a slightly modified optimal topology shown in Figure 35.

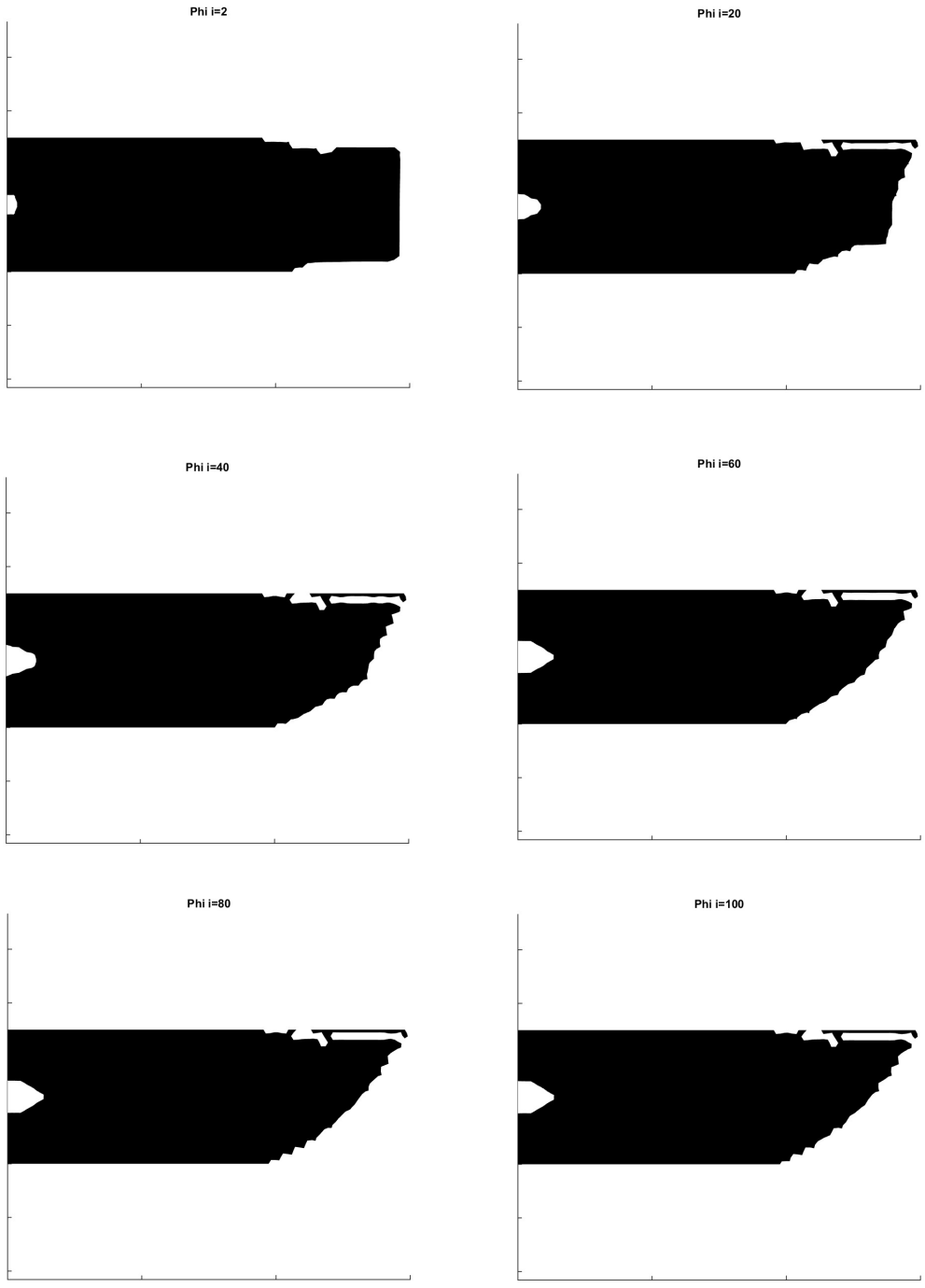

Figure 27: Evolution of ϕ in study 1 using the first set of boundary conditions, $Vol^* = 0.7$ and $\beta = 10^3$

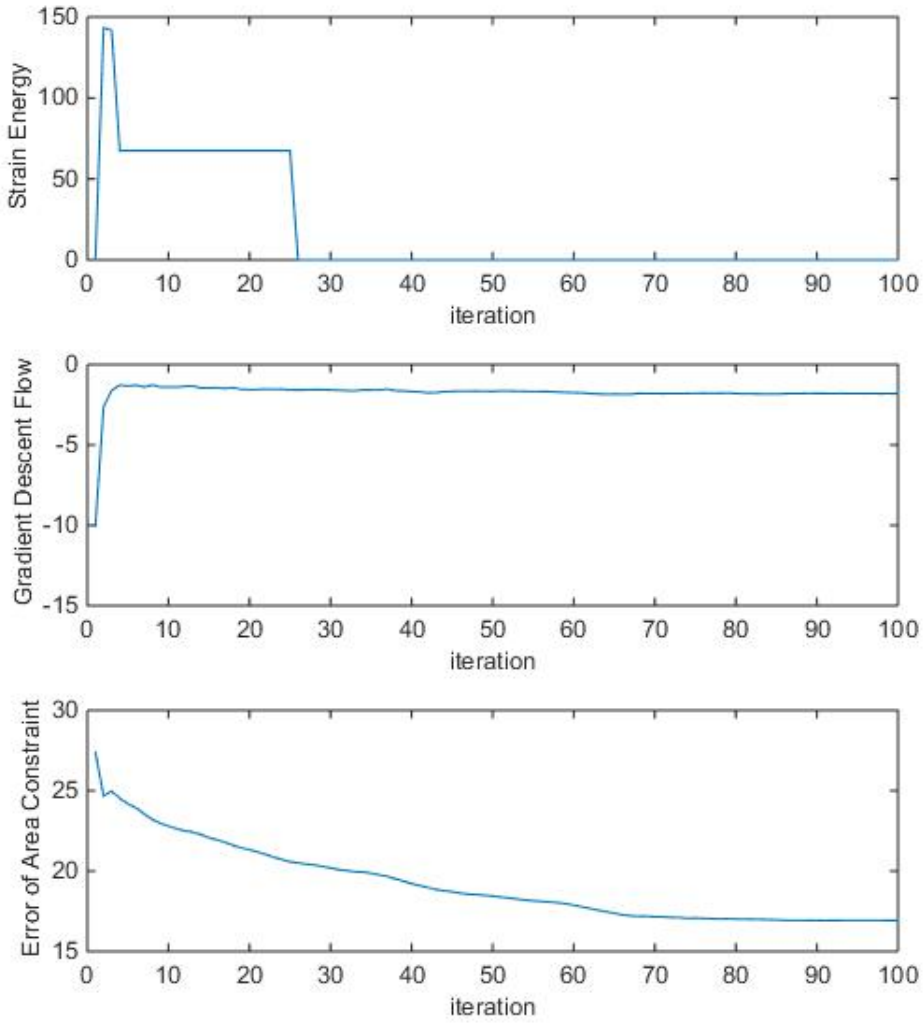

Figure 28: Performance of optimization procedure in study 1 using the first set of boundary conditions, $Vol^* = 0.7$ and $\beta = 10^3$

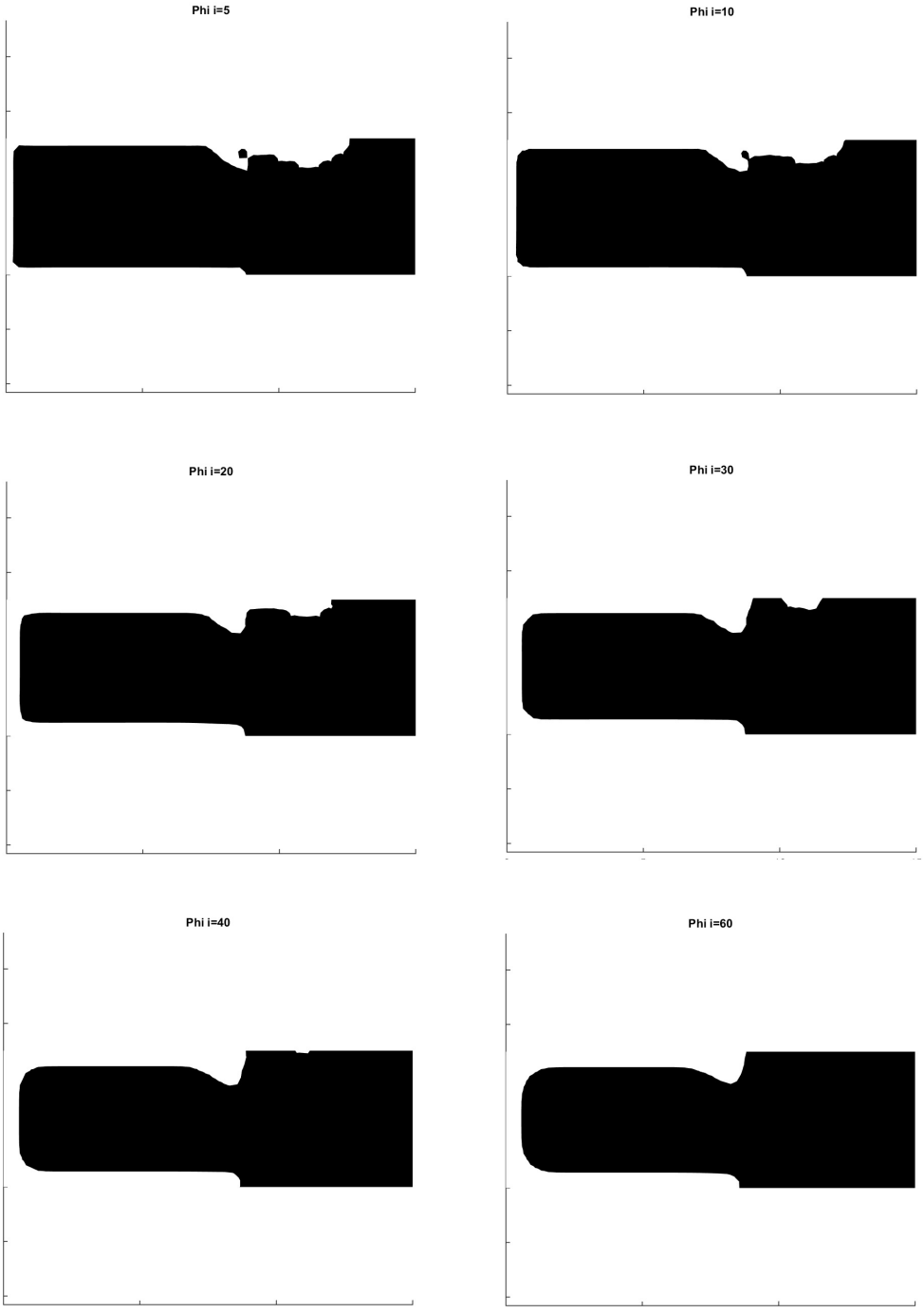

Figure 29: Evolution of ϕ in study 2 using the second set of boundary conditions, $Vol^* = 0.7$ and $\beta = 10^3$

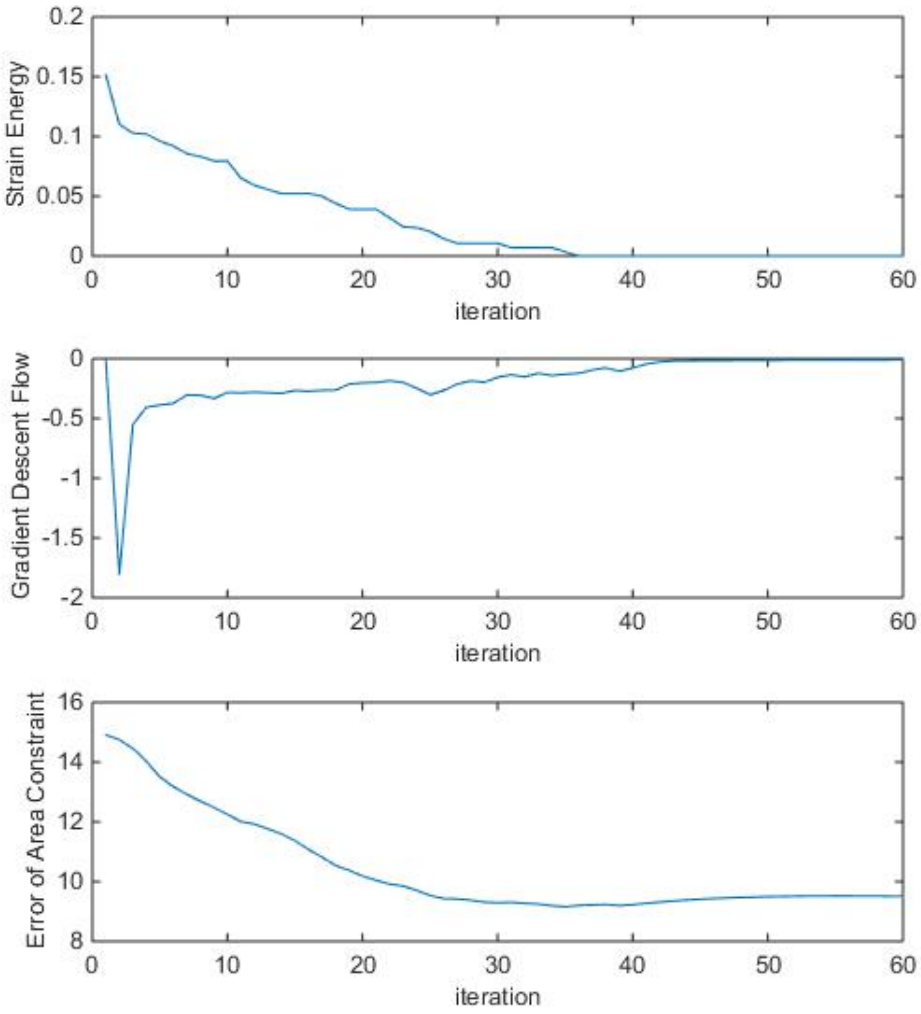

Figure 30: Performance of optimization procedure in study 2 using the second set of boundary conditions, $Vol^* = 0.7$ and $\beta = 10^3$

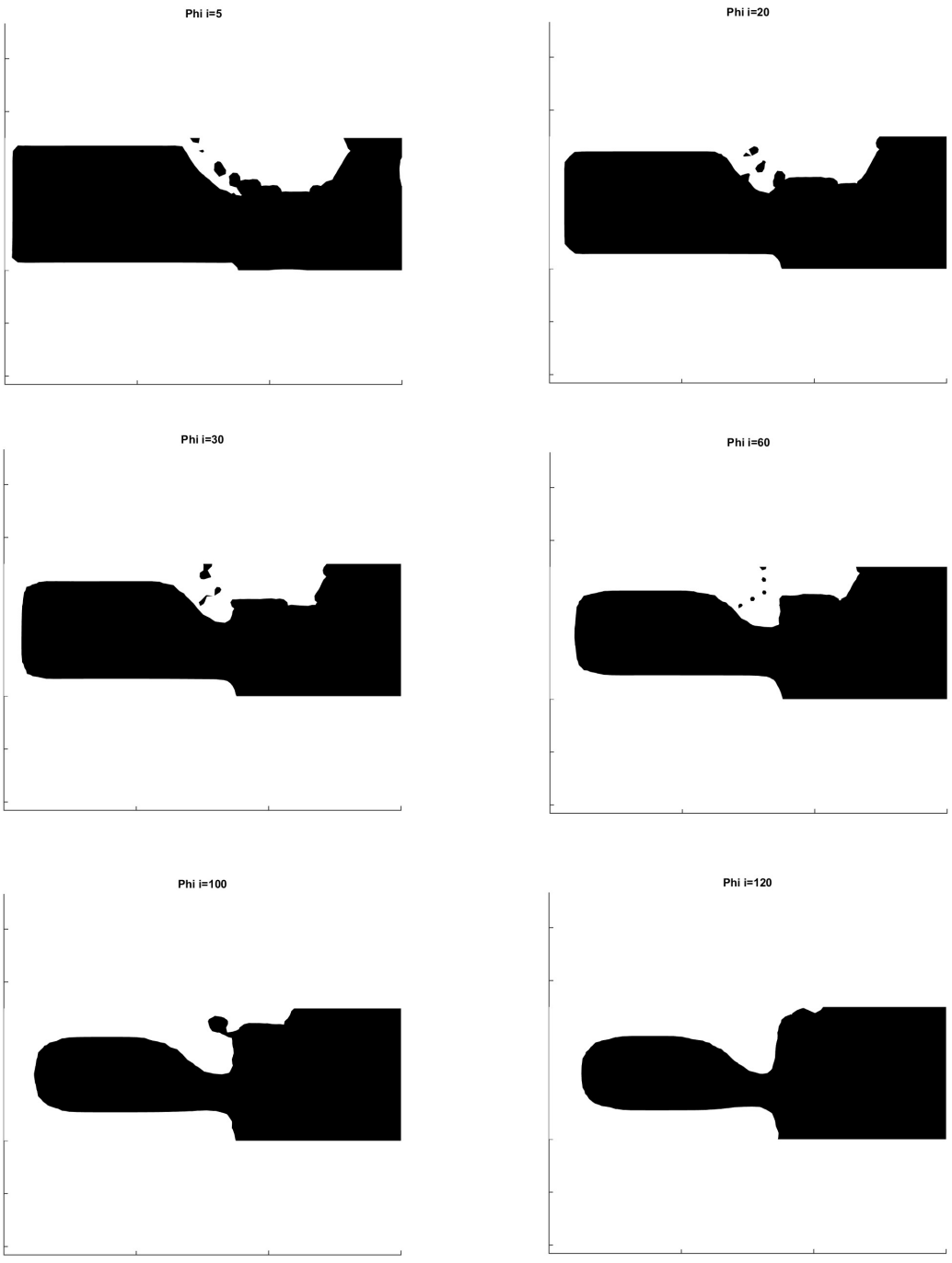

Figure 31: Evolution of ϕ in study 3 using the second set of boundary conditions, $Vol^* = 0.6$ and $\beta = 10^3$

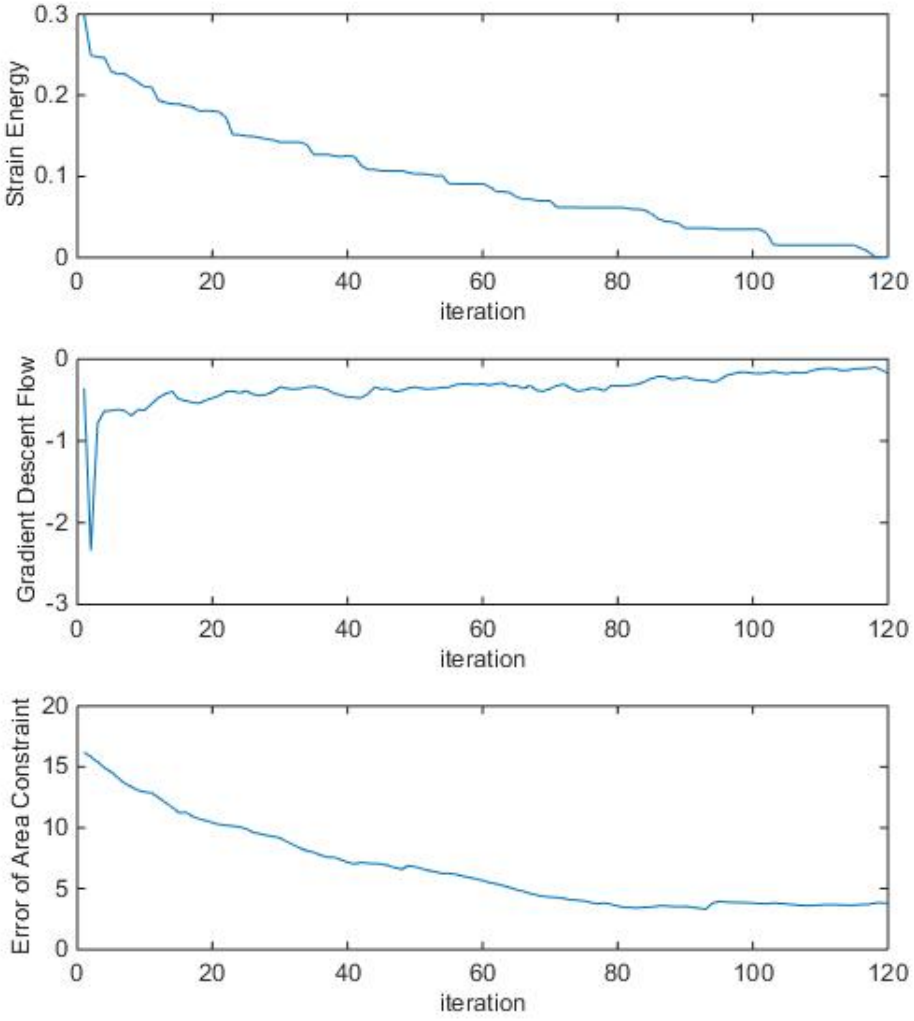

Figure 32: Performance of optimization procedure in study 3 using the second set of boundary conditions, $Vol^* = 0.6$ and $\beta = 10^3$

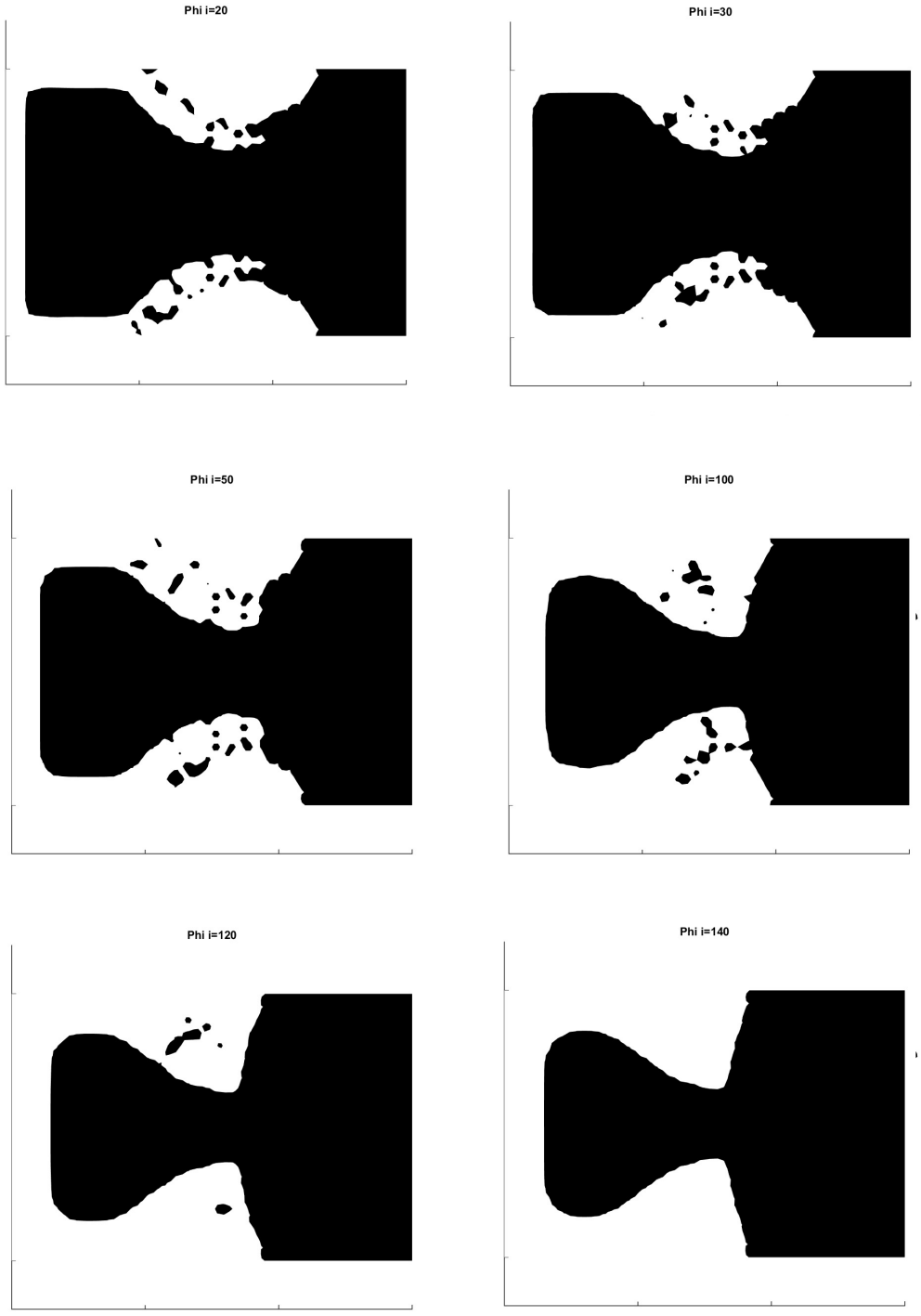

Figure 33: Evolution of ϕ in study 4 using the third set of boundary conditions, $Vol^* = 0.6$ and $\beta = 10^{-3}$

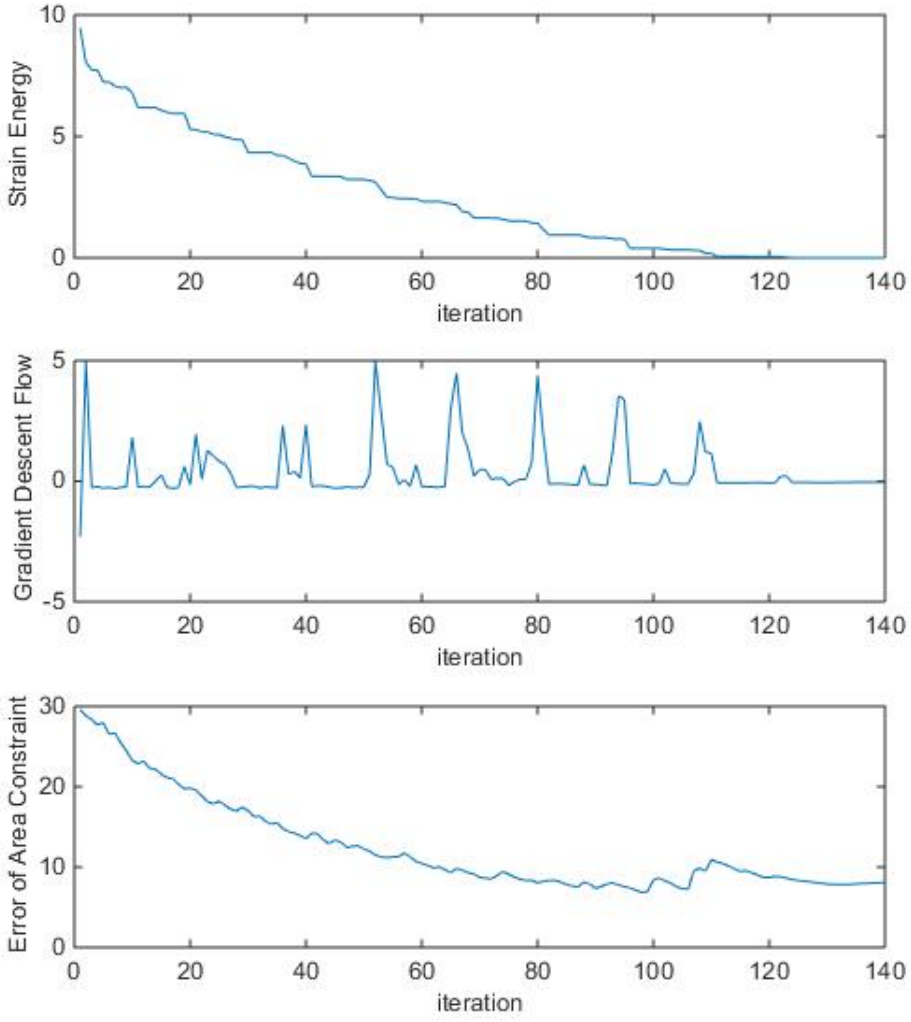

Figure 34: Performance of optimization procedure in study 4 using the third set of boundary conditions, $Vol^* = 0.6$ and $\beta = 10^{-3}$

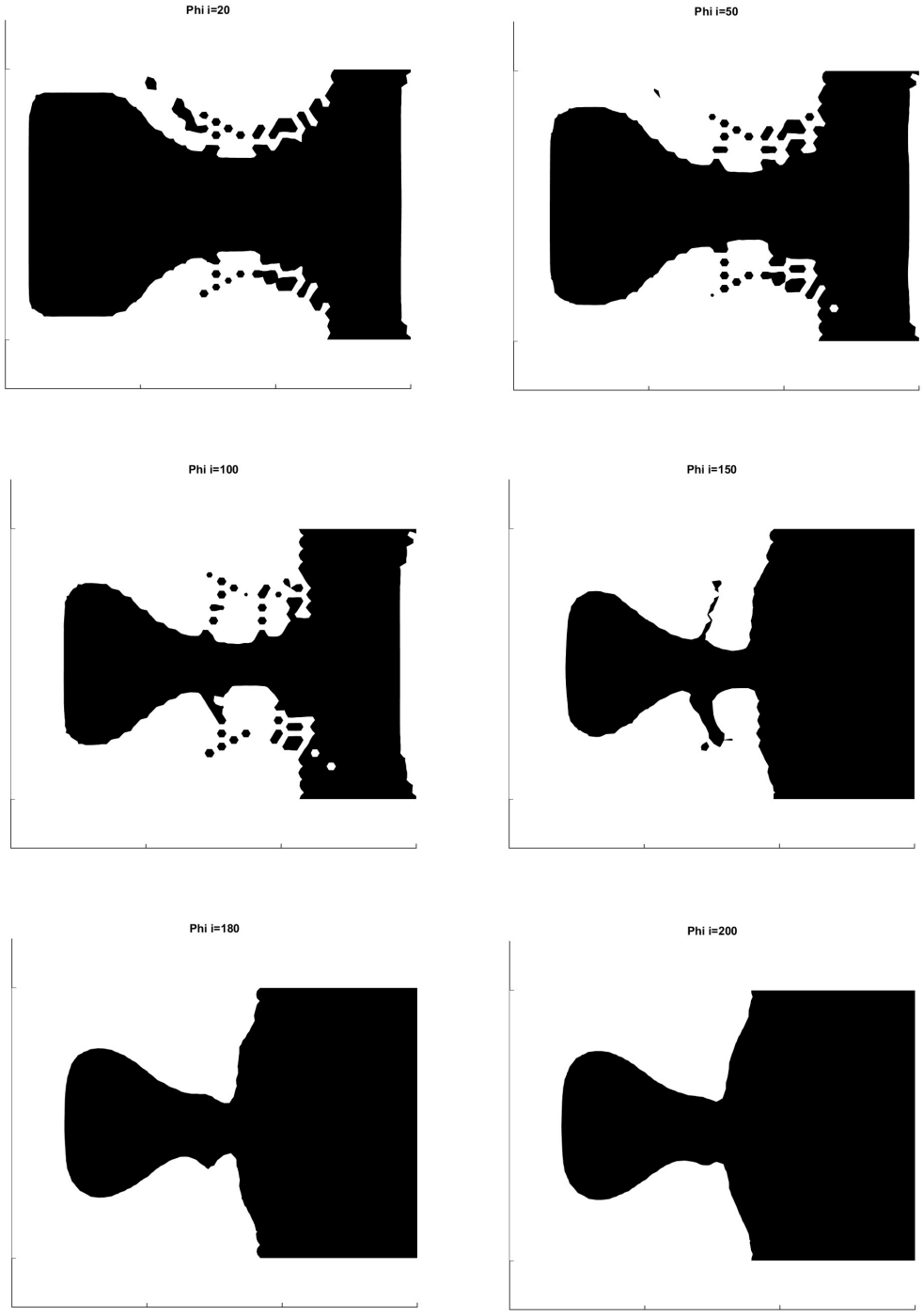

Figure 35: Evolution of ϕ in study 5 using the third set of boundary conditions, $Vol^* = 0.6$ and $\beta = 5 * 10^{-3}$

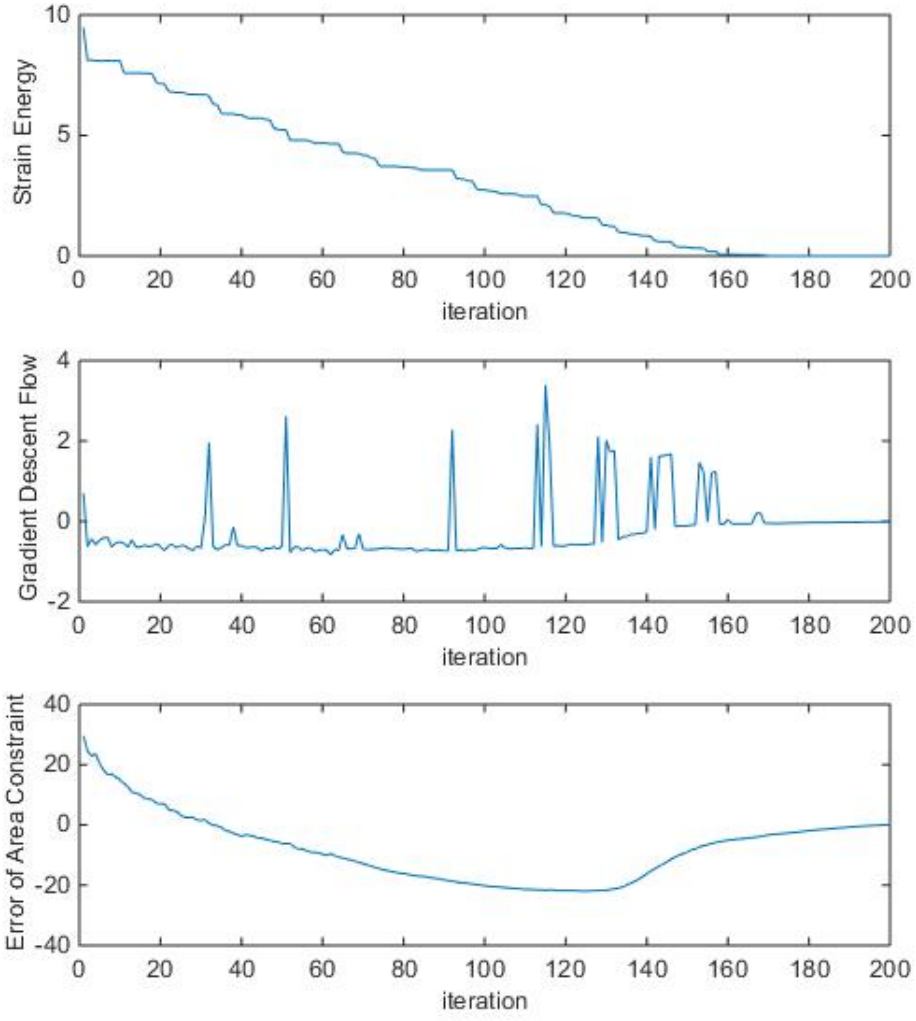

Figure 36: Performance of optimization procedure in study 5 using the third set of boundary conditions, $Vol^* = 0.6$ and $\beta = 5 * 10^{-3}$

5 Conclusions and Future Work

5.1 Conclusions

In this thesis, we applied a level-set based compliance minimization model on a bone scaffold generated based on mechano-regulatory algorithm. Mechano-regulatory simulation is working as promised in literature and successfully simulates the tissue differentiation in fracture gap. Results from topology optimization on the scaffold show that the optimization algorithm can be performed successfully on this case as it converges to an optimal solution, however, the volume constraint is not satisfied due to a high initial volume. Also a new boundary condition is suggested to avoid the barrier made by bone between the marrow canals on either sides of model. Unfortunately, this approach is not capable of controlling porosity of a porous material and results are quite contrasting from expected. Specifically, the mechano-regulatory algorithm has a strong tendency to fill the entire gap with the final tissue(bone) leaving no space for the earlier types of tissues. As a consequence, the converged solution is a solid structure lacking the porosity desired in a functional bone scaffold. Nevertheless this should not be considered as a major negligence as the proposed model is currently studying the cortical type of bone. Therefore, obtained solution can be manufactured as a primary scaffold filling the gap and assisting later stages of bone healing but cannot replace the bone itself.

5.2 Future Work

Although two models developed in this thesis, namely the mechano-regulatory model and the topology optimization design approach are working on their own as expected, the result of the integrated design framework suggests that updates to both models are needed to address bone scaffold design problems in a more effective way. These can be summarized as:

- The update of the mechano-regulatory model to incorporate biological functionality such as cell migration, proliferation and angiogenesis, etc.
- The update of the topology optimization model to address not only compliance but also biological functionality compatible with the mechano-regulatory model.
- Alternative integration of both models to mimic either bone, scaffold or both at the same time.
- Incorporation of manufacturability and additional functionality to both models as expected according to experimental studies in literature.

References

Allaire, G., De Gournay, F., Jouve, F., and Toader, A. (2005). Structural optimization using topological and shape sensitivity via a level set method. *Control and cybernetics*, 34(1):59.

Aro, H. T. and Chao, E. Y. (1993). Bone-healing patterns affected by loading, fracture fragment stability, fracture type, and fracture site compression. *Clinical orthopaedics and related research*, 293:8–17.

Bathe, K.-J. (2006). *Finite element procedures*. Klaus-Jurgen Bathe.

Bendsøe, M. P. (1989). Optimal shape design as a material distribution problem. *Structural optimization*, 1(4):193–202.

Bendsøe, M. P. and Kikuchi, N. (1988). Generating optimal topologies in structural design using a homogenization method. *Computer methods in applied mechanics and engineering*, 71(2):197–224.

Bendsøe, M. P. and Sigmund, O. (1999). Material interpolation schemes in topology optimization. *Archive of applied mechanics*, 69(9-10):635–654.

Claes, L. E., Heigele, C. A., Neidlinger-Wilke, C., Kaspar, D., Seidl, W., Margevicius, K. J., and Augat, P. (1998). Effects of mechanical factors on the fracture healing process. *Clinical orthopaedics and related research*, 355:S132–S147.

Cowin, S. C. (1999). Bone poroelasticity. *Journal of biomechanics*, 32(3):217–238.

Goodship, A. and Kenwright, J. (1985). The influence of induced micromovement upon the healing of experimental tibial fractures. *Bone & Joint Journal*, 67(4):650–655.

Goodship, A. E., Cunningham, J. L., and Kenwright, J. (1998). Strain rate and timing of stimulation in mechanical modulation of fracture healing. *Clinical orthopaedics and related research*, 355:S105–S115.

Hollister, S. J. (2005). Porous scaffold design for tissue engineering. *Nature materials*, 4(7):518–524.

Hollister, S. J., Maddox, R., and Taboas, J. M. (2002). Optimal design and fabrication of scaffolds to mimic tissue properties and satisfy biological constraints. *Biomaterials*, 23(20):4095–4103.

Hughes, T. J. (2012). *The finite element method: linear static and dynamic finite element analysis*. Courier Corporation.

Huiskes, R., Van Driel, W., Prendergast, P., and Søballe, K. (1997). A biomechanical regulatory model for periprosthetic fibrous-tissue differentiation. *Journal of materials science: Materials in medicine*, 8(12):785–788.

Kenwright, J. and Gardner, T. (1998). Mechanical influences on tibial fracture healing. *Clinical orthopaedics and related research*, 355:S179–S190.

Kutz, M. (2003). *Standard handbook of biomedical engineering and design*. McGraw-Hill.

Lacroix, D., Prendergast, P., Li, G., and Marsh, D. (2002). Biomechanical model to simulate tissue differentiation and bone regeneration: application to fracture healing. *Medical and Biological Engineering and Computing*, 40(1):14–21.

Liu, Z., Korvink, J. G., and Huang, R. (2005). Structure topology optimization: fully coupled level set method via femlab. *Structural and Multidisciplinary Optimization*, 29(6):407–417.

Michell, A. G. M. (1904). Lviii. the limits of economy of material in frame-structures. *The London, Edinburgh, and Dublin Philosophical Magazine and Journal of Science*, 8(47):589–597.

Osher, S. and Sethian, J. A. (1988). Fronts propagating with curvature-dependent speed: algorithms based on hamilton-jacobi formulations. *Journal of computational physics*, 79(1):12–49.

Osher, S. J. and Santosa, F. (2001). Level set methods for optimization problems involving geometry and constraints: I. frequencies of a two-density inhomogeneous drum. *Journal of Computational Physics*, 171(1):272–288.

Prendergast, P., Huiskes, R., and Søballe, K. (1997). Biophysical stimuli on cells during tissue differentiation at implant interfaces. *Journal of biomechanics*, 30(6):539–548.

Rémond, A., Naïli, S., and Lemaire, T. (2008). Interstitial fluid flow in the osteon with spatial gradients of mechanical properties: a finite element study. *Biomechanics and modeling in Mechanobiology*, 7(6):487–495.

Rozvany, G. (1972a). Grillages of maximum strength and maximum stiffness. *International Journal of Mechanical Sciences*, 14(10):651–666.

Rozvany, G. (1972b). Optimal load transmission by flexure. *Computer Methods in Applied Mechanics and Engineering*, 1(3):253–263.

Rozvany, G. (1998). Exact analytical solutions for some popular benchmark problems in topology optimization. *Structural optimization*, 15(1):42–48.

Rozvany, G. (2001). Aims, scope, methods, history and unified terminology of computer-aided topology optimization in structural mechanics. *Structural and Multidisciplinary Optimization*, 21(2):90–108.

Sethian, J. A. and Wiegmann, A. (2000). Structural boundary design via level set and immersed interface methods. *Journal of computational physics*, 163(2):489–528.

Yao, W., Li, Y., and Ding, G. (2012). Interstitial fluid flow: the mechanical environment of cells and foundation of meridians. *Evidence-Based Complementary and Alternative Medicine*, 2012.

Zhang, D., Weinbaum, S., and Cowin, S. (1998). Estimates of the peak pressures in bone pore water. *Journal of biomechanical engineering*, 120(6):697–703.

Zhao, H.-K., Chan, T., Merriman, B., and Osher, S. (1996). A variational level set approach to multiphase motion. *Journal of computational physics*, 127(1):179–195.

Zienkiewicz, O. C., Taylor, R. L., Zienkiewicz, O. C., and Taylor, R. L. (1977). *The finite element method*, volume 3. McGraw-hill London.

6 Appendix

6.1 Topology Otimization Code

```
% ADDING COMSOL CLASSES
import com.comsol.model.*
import com.comsol.model.util.*
ModelUtil.clear % Clear all models on the server

% LOADING MODEL
fileName='TOPScript';
model =mphload(fileName);

% INITIALIZATION
model.sol('sol1').clearSolution();
model.sol('sol4').clearSolution();

%PARAMETERS:
beta=-1e-2;
i=1; % indexing variable
fig1=figure('Name','Phi');
t=0;
t_step=0.3;

```

```
% MESHING
model.mesh('mesh1').run;

% SOLUTION
disp('      time          t_step          compliance      energy')
tstart=tic;
while(i <=100)
    if(i==1)
        % This part is to initialize the level-set surface
        model.study('std3').feature('stat').set('usesol','on');
        model.study('std3').feature('stat').set('notsolmethod','init');
        model.study('std3').feature('stat').set('notstudy','zero');
    elseif(i==2)
        % To receive the level-set surface from time-dependent study
        model.study('std3').feature('stat').set('notsolmethod','sol');
        model.study('std3').feature('stat').set('notstudy','std2');
        model.study('std3').feature('stat').set('notsolnum','last');
    end

    % RUN SOLID MECHANICS
    model.study('std3').run();
    pause(1);
    figure(fig1);
```

```
44      pd_tot{i}=mphplot(model,'pg1','rangenum',1); % Plot phi
45      colorbar('off')
46      title(['Phi i=',num2str(i)]);
47      saveas(fig1,sprintf('Phi%d.png',i));
48
49      % GETTING VALUES FROM COMSOL
50      area=mphint2(model,'root.step2(phi)','surface','Dataset',
            mechDatSet,'Intorder',4,'Intvolume','on','Method','
            integration','Selection',[1]);
51      lm_area=mphint2(model,'root.step2(phi)-0.5','surface','
            Dataset',mechDatSet,'Intorder',4,'Intvolume','on','
            Method','integration','Selection',[1]);
52      Area_Error(i)=lm_area;
53      penalty_term=beta*(lm_area);
54      lambda_num=mphint2(model,'energy*(DiracDelta(phi))*Rbf(
            phi,hmesh_max)*min(gradmax,mag_gradphi)','surface','
            Dataset',mechDatSet,'Intorder',4,'Intvolume','on','
            Method','integration','Selection',[1]);
55      lambda_den=mphint2(model,'(DiracDelta(phi))*Rbf(phi,
            hmesh_max)*min(gradmax,mag_gradphi)','surface','
            Dataset',mechDatSet,'Intorder',4,'Intvolume','on','
            Method','integration','Selection',[1]);
56      lambda=-1*lambda_num/lambda_den;
57      lambda_tot(i)=lambda;
58      SEnergy=mphint2(model,'0.5*(solid.eX^2+solid.eY^2+(1-
            solid.nu)*solid.eXY^2+2*solid.eX*solid.eY*solid.nu)
            /(1-solid.nu^2)','surface','Dataset',mechDatSet,'
            Intorder',4,'Intvolume','on','Method','integration','
            Selection',[1]);
59      SEnergy_tot(i)=SEnergy;
```

```
60      GradientDescent=mphint2(model,'((solid.eX^2+solid.eY
            ^2+(1-solid.nu)*solid.eXY^2+2*solid.eX*solid.eY*solid.
            nu)/(1-solid.nu^2)+lambda2)*Rbf(phi,hmesh_max)*min(
            gradmax,mag_gradphi)','surface','Dataset',mechDatSet,'
            Intorder',4,'Intvolume','on','Method','integration','
            Selection',[1]);
61      GradientDescent_tot(i)=GradientDescent;
62
63      % SENDING VALUES TO COMSOL
64      model.variable('var1').set('penalty_term',num2str(
            penalty_term,5));
65      model.variable('var1').set('lambda_top', num2str(
            lambda_num,5));
66      model.variable('var1').set('lambda_bot', num2str(
            lambda_den,5));
67      model.variable('var1').set('lambda2', num2str(lambda,5));
68
69      % RUN HAMILTON JACUBI
70      model.study('std2').run();  % Run time-dependent module
71
72      i=i+1; % Increment i
73      t=t+t_step; % Increment time
74  end
75
76  % PLOTTING
77  figure
78  subplot(3,1,2)
79  plot(GradientDescent_tot)
80  xlabel('iteration','FontSize',10)
81  ylabel('Gradient Descent Flow','FontSize',10)
```

```
82
83 subplot(3,1,1)
84 plot(SEnergy_tot)
85 xlabel('iteration','FontSize',10)
86 ylabel('Strain Energy','FontSize',10)
87
88 subplot(3,1,3)
89 plot(Area_Error)
90 xlabel('iteration','FontSize',10)
91 ylabel('Error of Area Constraint','FontSize',10)
92
93 % SAVING RESULTS IN COMSOL
94 mphsave(model,fileName);
```

6.2 Mechano-regulatory Code

```
% ADDING COMSOL CLASSES
import com.comsol.model.*
import com.comsol.model.util.*

% LOADING MODEL
fileName='V2Script.mph';
model=mphload(fileName);
model.sol('sol1').clearSolution();
DatSet='dset1';


model.study('std1').feature('time').set('plot', 'on');
model.study('std1').run();
pause(1);

for i=1:8
    if i==1
    %    Granulation Tissue (mat4)
    model.material('mat8').selection.set([]);
    model.material('mat4').selection.set([1]);
    elseif i==2
    %    Evolving Tissue (mat8)
    model.material('mat4').selection.set([]);
    model.material('mat8').selection.set([1]);
    end

model.study('std1').run();

```

```
fig1=figure();
plotStimuli=mphplot(model,'pg7','rangenum',2);
fig2=figure();
plotTissue=mphplot(model,'pg8','rangenum',2);

model.result.export('data1').set('descr', {''});
model.result.export('data1').set('expr', {'Stimuli'});
model.result.export('data1').set('filename', 'C:\Users\Bahari
    \Documents\Mechano v5\Stim.txt');
model.result.export('data1').set('solnum', {'1'});
model.result.export('data1').set('unit', {'1'});
model.result.export('data1').set('solnum', {'11'});
model.result.export('data1').run;

model.func.remove('int1');
model.func.create('int1', 'Interpolation');
model.func('int1').model('mod1');
model.func('int1').set('source', 'file');
model.func('int1').set('filename', 'C:\Users\Bahari\Documents
    \Mechano v5\Stim.txt');
model.func('int1').label('StimInt');
model.func('int1').set('argunit', 'm,m');

end
```